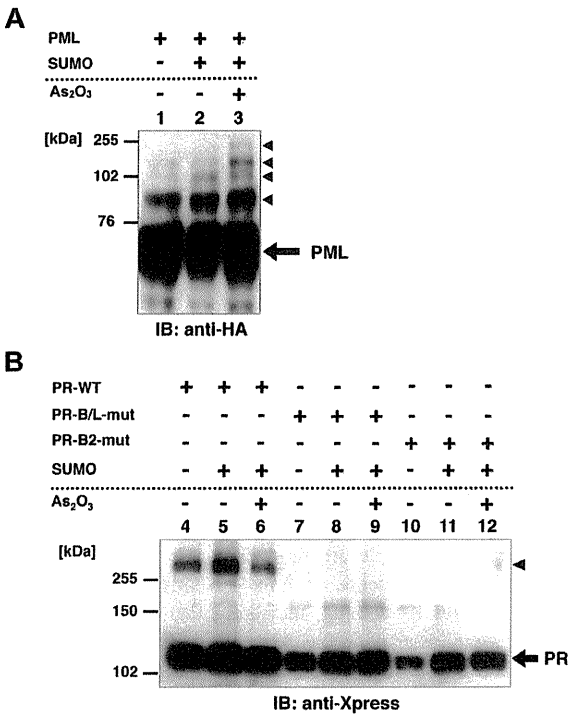

Figure 3. Posttranslational modification of PML, PR-WT, PR-B/L-mut, and PR-B2-mut induced by SUMO1/Ubc9. (A) HA-tagged PML and SUMO1/Ubc9 (SUMO) expression vectors were transfected into HeLa cells as indicated and incubated with or without As_2O_3 (10μM) for 8 hours. Immunoblot analysis using an anti-HA antibody was carried out. Black arrowheads indicate SUMO-modified PML. (B) Xpress-tagged PR-WT, PR-B/L-mut, or PR-B2-mut was overexpressed in HeLa cells with or without SUMO1/Ubc9 and incubated with or without As_2O_3 (10μM) for 8 hours. Black arrowhead indicates SUMO-modified/dimerized PR-WT (lanes 4-6). Note that the modified bands of PR-B/L-mut and PR-B2-mut were barely detected (lanes 7-12).

the presence of As_2O_3 (Figure 6Bv,vi,viii). These data strongly suggest that the L218P mutation in the PML-B2 domain contributes to the aberrant PML body formation and disrupts responsiveness to As_2O_3 treatment.

Cellular localization of endogenous PR-B/L-mut without As_2O_3 in primary cells from a patient

To show the localization of PR-WT and PR-B/L-mut protein in primary leukemia cells, IF staining using an anti-PML antibody was performed (Figure 7). Primary leukemia cells from patient 1 obtained at diagnosis and at the terminal stage were used to detect PR-WT and PR-B/L-mut, respectively. Nearly the same localization pattern as seen in Figure 5 was confirmed in this assay. The PML bodies were observed as a granular pattern at diagnosis (PR-WT), but the pattern was significantly altered to become diffuse at the terminal stage (PR-B/L-mut). These data strongly suggest that PR-B/L-mut protein was expressed and functional in primary leukemia cells, and may contribute to different responsiveness to As_2O_3 treatment.

Discussion

In the present study, we have shown acquired missense mutations in *PML-RARA* that are closely related to resistance to As_2O_3 treatment. In 2 patients, we detected A216V and L218P substitutions in the B2 domain of PML. The B2 domain is part of the RBCC motif, which is thought to be critical for PML homo/

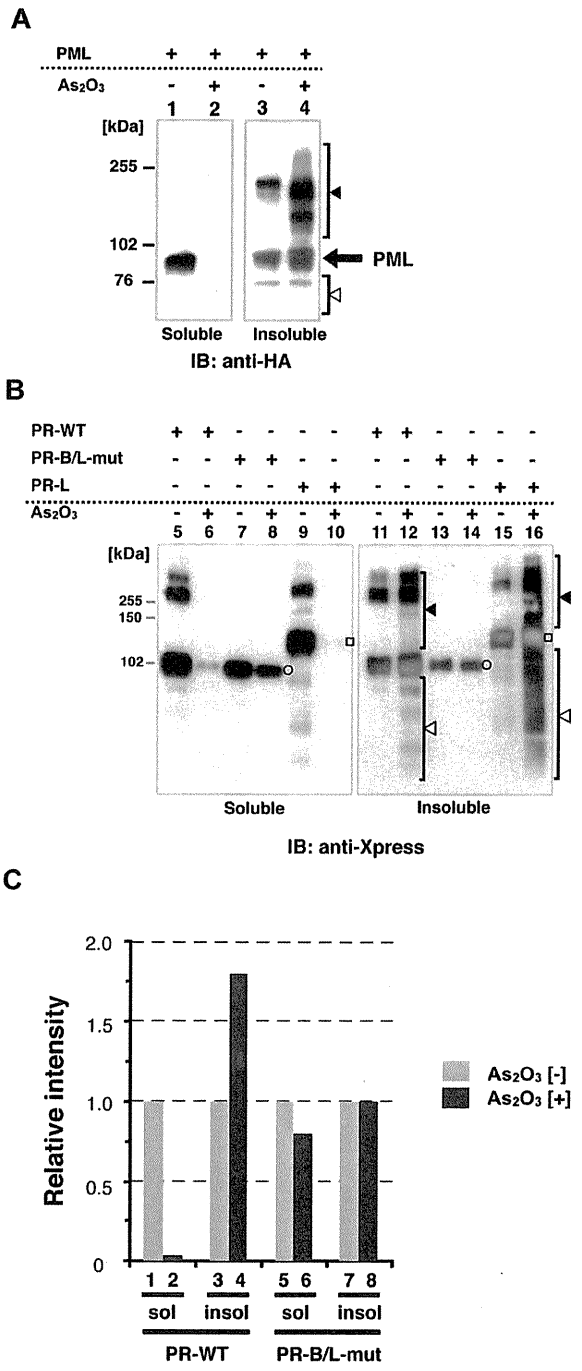

Figure 4. Protein localization of PML and its fusion proteins in soluble and/or insoluble fractions with or without As_2O_3. (A) HA-PML was overexpressed in HeLa cells with or without As_2O_3 (10μM for 2 hours), and the whole-cell lysate (soluble) and pellets (insoluble fraction) were obtained for immunoblotting. Black and white arrowheads indicate modified/oligomerized and degraded PML, respectively. (B) The same assay described in panel A was performed using PR-WT, PR-B/L-mut, and the long form of PML-RARA (PR-long). White circles indicate PR-WT or PR-B/L-mut and white squares indicate PR-long protein. Black and white arrowheads indicate modified/oligomerized and degraded fusion proteins, respectively. Note that neither protein transportation from the soluble to insoluble fraction (lanes 7 vs 8 and 13 vs 14) nor modified/oligomerized or degraded proteins after treatment with As_2O_3 (lanes 8 and 14) were observed with PR-B/L-mut. (C) Protein expression levels in panel B were measured using BioMax 1D software, and the relative intensity is depicted as a bar graph.

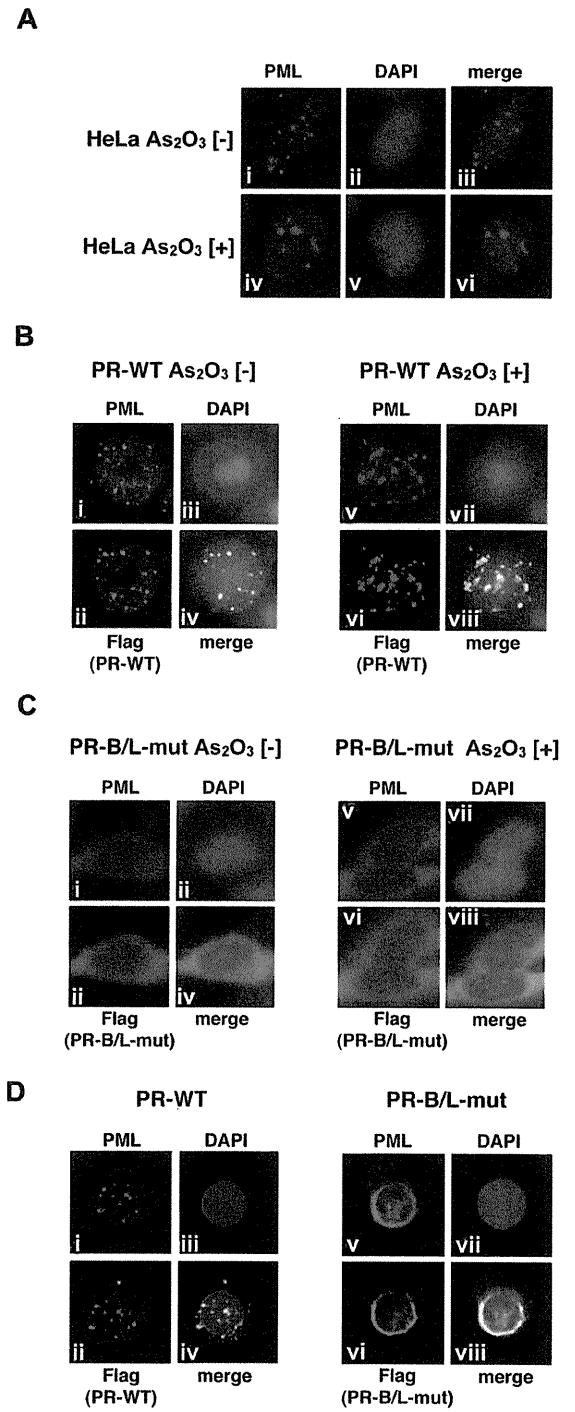

Figure 5. Analyses of the protein localization of PML, PR-WT, and PR-B/L-mut using IF staining. (A) HeLa cells were incubated with or without As_2O_3 (10μM) for 8 hours, and endogenous PML was detected with an anti-PML antibody. PML nuclear bodies were detected in green. The nuclei were stained with 4,6 diamidino-2-phenylindole (DAPI; blue). Note that the microgranular pattern of NBs without As_2O_3 (i and iii) was altered to become a macrogranular pattern with As_2O_3 (iv and vi). (B) Flag-tagged PR-WT was used for the same assay as described in panel A. Anti-FLAG and anti-PML antibodies were used to detect PR-WT and endogenous PML, respectively. PML bodies were confirmed in the cytoplasm with a microgranular pattern without As_2O_3 (i,ii, and iv) and a macrogranular pattern with As_2O_3 (v,vi, and viii). (C) When using Flag-tagged PR-B/L-mut, localization showed a diffuse pattern mostly in the cytoplasm with and without As_2O_3. (D) Flag-tagged PR-WT or PR-B/L-mut was overexpressed in U937 cells without As_2O_3, and the same IF staining was performed. Note that PR-B/L-mut localization was confirmed in the cytoplasm as a diffuse pattern. Magnification is 800×.

heterodimerization, oligomerization, and As_2O_3 binding.[23-25,34] Recent studies have indicated that As_2O_3 binds directly to cysteine residues in zinc fingers in the RBCC domain, especially C77/80 and C88/91 in the RING domain[24] and C212 and C213 in the B2 domain.[25] Binding of As_2O_3 in the RBCC domain appears to be critical for the effect of As_2O_3 on PML-RARA.[24,25] Interestingly, the mutations described herein were located just adjacent to the CC motif (C212/213) in the B2 domain, which is thought to be critical for As_2O_3 binding (Figure 1D). These findings suggest that substitutions at A216 and L218 may affect proper As_2O_3 binding, resulting in aberrant responsiveness to As_2O_3 through aberrant subcellular localization, insufficient SUMOylation, and/or multimerization.

The in vitro SUMOylation assay indicated that PR-B/L-mut and PR-B2-mut mostly lack SUMO1-Ubc9–induced SUMOylation and dimerization/multimerization (Figure 3B), and this was not changed in the presence of As_2O_3. It has been suggested that degradation of the PML-RARA protein with As_2O_3, followed by SUMOylation and oligomerization,[24,25] may also be inhibited by mutations in the B2 domain. Furthermore, PR-B/L-mut was localized in both the soluble and insoluble fractions, and the localization was not changed in the presence of As_2O_3. Nearly the same result was obtained with IF staining, indicating that PR-B/L-mut and PR-B2-mut were localized in the cytoplasm with a diffuse pattern that was not altered in the presence of As_2O_3 (Figure 5C). Furthermore, PR-L-B2-mut2 was localized in the nucleus as a diffuse pattern with or without As_2O_3 (Figure 6B). These results strongly suggest that amino acid substitution in the B2 domain is

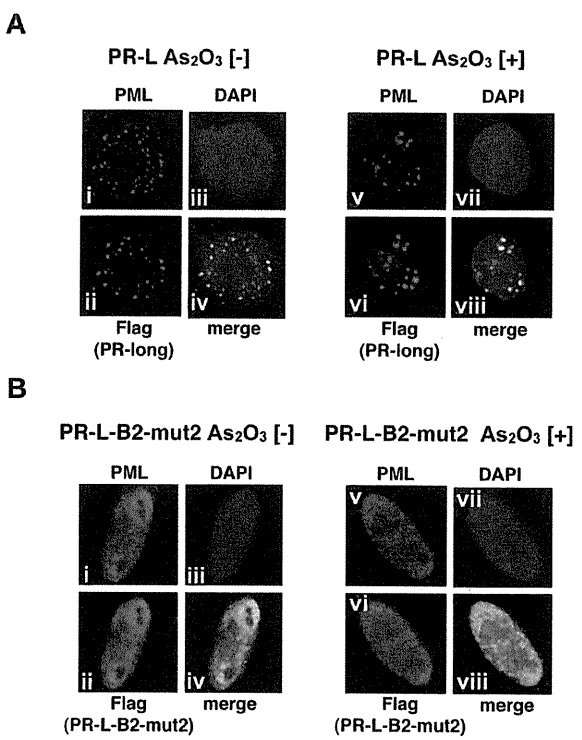

Figure 6. Analyses of the protein localization of PR-L and PR-L-B2-mut2 using IF staining. (A) Flag-tagged PR-L was overexpressed in HeLa cells with or without As_2O_3. Anti-FLAG and PML antibodies were used to detect PR-L and endogenous PML, respectively. PML bodies were confirmed in the nucleus with a microgranular pattern without As_2O_3 (i,ii, and iv) and a macrogranular pattern with As_2O_3 (v,vi, and viii). (B) A similar assay was performed using PR-L-B2-mut2. Note that the localization of PR-L-B2-mut2 was confirmed in the nucleus as a diffuse pattern with or without As_2O_3.

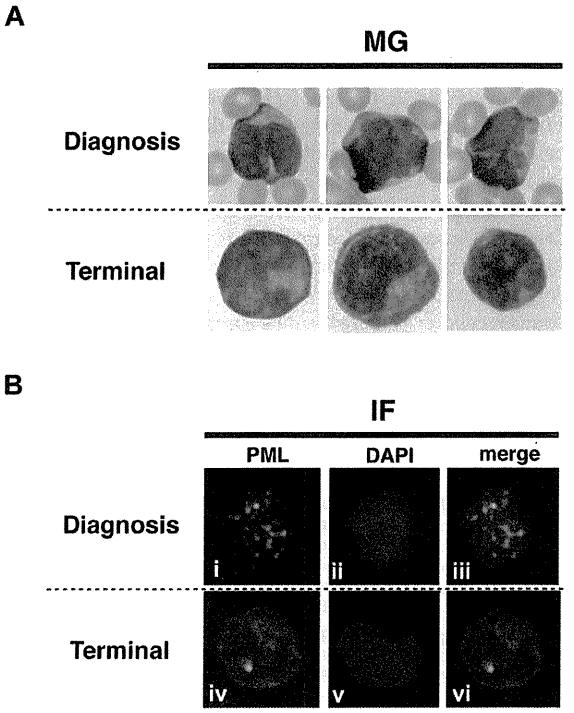

Figure 7. Protein localization of PML and its fusion proteins in primary leukemia cells from patient #1. May-Giemsa (MG) staining (A) and IF staining (B) are shown. The primary leukemia cells from patient 1 were obtained at diagnosis and at the terminal stage (shown as 1 and 5, respectively, in Figure 1A) and were used in this assay. PML nuclear bodies can be observed in the cells at diagnosis (i and iii), but at the terminal stage, PML and its fusion proteins were observed in the cytoplasm showing a diffuse pattern (iv and vi).

critical for the aberrant responsiveness in vitro, and the mutations may be critical for the resistance to As_2O_3 therapy in vivo.

In patient 6, only 2 of 20 clones (10%) contained a genetic mutation resulting in an L218P substitution in the B2 domain of the PML region. The genetic mutation was theoretically present in 20% of bone marrow cells, and the remaining 77% of leukemia cells (*PML-RARA*–positive cells [97.1%] in FISH analysis included *PML-RARA*–mutated cells [20%]) harbored wild-type PML-RARA according to the FISH analysis. Careful evaluation of whether the mutation contributes to clinical resistance to As_2O_3 therapy should be performed. Because clinically refractory disease against As_2O_3 was confirmed after the bone marrow aspiration, clonal expansion of PML-RARA with the L218P substitution may have been related to the insufficient responsiveness to As_2O_3 therapy. Another question is when the mutated clone appeared in this patient. One possibility is that the mutated clone was already present at the early stage of the disease. Genetic analysis using DNA obtained at the disease onset may be useful for clarifying this. Unfortunately, DNA obtained at the disease onset and the terminal stage of this patient was not available, and clarifying these issues is not currently possible. Further examination of additional patients and genetic analyses of samples obtained at several time points during the disease progression are required.

Interestingly, PR-B/L-mut was localized in the cytoplasm (Figures 5C and 6B), not in the nucleus. As reported previously, an NLS on the PML C-terminus is critical for transport into the nucleus.[35,36] The absence of an NLS motif in the short form of PML-RARA (bcr3)[32,37,38] may explain the cytoplasmic localization of PR-WT and PR-B/L-mut in our study. Furthermore, PR-B/L-mut and -B2-mut showed a diffuse pattern (Figures 5C-D, 6B, and 7B). Borden et al[34] reported that substitution of conserved zinc finger domains in B1 and/or B2 disrupts PML nuclear body formation in vivo, and they also suggested that B1/B2 domains may be involved in the homo/hetero-oligomerization process via protein-protein interactions. Other studies have indicated that PML-RARA with mutations in B2 show a diffuse cytoplasmic pattern, perhaps because the mutated proteins cannot bind to nuclear body–forming proteins such as Daxx, Sp100, and SUMO-1, resulting in a failure to accumulate in the nuclear body.[24,25,39,40] Amino acid substitution near the zinc finger motif in the B2 domain may lead to conformational changes in the PML protein. Further analyses are needed.

PR-B/L-mut also contains a mutation in the LBD of RARA (G391E). Previous studies have indicated that the LBD mutation is closely related to ATRA resistance,[41-44] and patient 1 in this study also showed a clinically refractory response to ATRA in the late stage of his disease progression and resistance to Am80 in the terminal stage. The LBD mutation G391E was detected only in the terminal stage (Figure 2B lanes 4 and 5). Therefore, an APL variant phenotype with bcr3 of the PML-RARA protein may be related to a poor prognosis,[32,37,38] showing that insufficient ATRA effectiveness and the LBD mutation are related to a consistent phenotype of ATRA resistance.[45] PR-B/L-mut is localized mainly in the cytoplasm, and the effectiveness of ATRA may not be anticipated. The function of PR-WT and PR-B/L-mut as transcription factors to control activation and/or repression by recruiting coregulators, such as p300/CBP, SMRT/N-CoR-TBL1/R1, and histone deacetylases,[26,29,46,47] should be analyzed to confirm the responsiveness to ATRA. Conversely, the probability of the effects of the LBD mutation on As_2O_3 resistance may be relatively low based on our experiment, because the diffuse localization pattern in the cytoplasm of PR-B2-mut without an LBD mutation in the presence or absence of As_2O_3 showed nearly the same pattern as PR-B/L-mut (data not shown). Furthermore, a previous study indicated that ATRA-resistant NB4 clones with mutations in the PML-RARA LBD domain were fully sensitive to As_2O_3 treatment.[48]

Interestingly, leukemia cells from patient 1 contained minor clones of PR-B2-mut and PR-LBD-mut in addition to the major clone of PR-B/L-mut at the terminal stage (Figure 2B time points 4 and 5), which is difficult to explain. One possibility is that one allele of the wild-type *PML* and *RARA* genes originally had genetic mutations in the B2 and LBD domains, and PR-WT, PR-B2-mut, PR-LBD-mut, and PR-B/L-mut were generated at the early stage of disease progression. Another explanation is that the *PML-RARA* fusion gene with mutations in the B2 and LBD domains translocated again with wild-type *PML* or *RARA* genes during the disease progression. Further analyses are required using several strategies including allele-specific PCR, FISH, and/or single nucleotide polymorphism analysis.

Mutations in the B2 domain that result in insufficient responsiveness to As_2O_3 therapy were confirmed in 2 of 15 (13%) patients with APL treated with As_2O_3. Recently, As_2O_3 was introduced as a consolidation treatment, and the event-free survival at 3 years was significantly improved compared with conventional consolidation treatment with ATRA and daunorubicin (80% vs 63%).[12] However, almost 5% of patients with APL treated with As_2O_3 show As_2O_3 refractory disease.[49] Because it is possible that a PML B2 mutation may be partly related to the As_2O_3 refractory phenotype, repeated genetic analyses at several time points of the clinical course may be useful for predicting patients at high risk for a poor

response to As_2O_3 therapy. Further investigation is required to confirm the clinical significance.

Acknowledgments

The authors thank Nobuhiko Emi, Kazuhito Yamamoto, Yukiyasu Ozawa, Taku Kimura, Keiko Niimi, Hiroshi Sao, Kazunori Ohnishi, and Hidehiko Saito for caring for the patients with APL and Tomoka Wakamatsu, Eriko Ushida, Manami Kira, Mari Otsuka, and Yukie Konishi for valuable laboratory assistance.

This work was supported by grants-in-aid for scientific research from the Ministry of Education, Culture, Sports, Science and Technology, Japan, and from the Public Trust Haraguchi Memorial Cancer Research Fund, Japan.

Authorship

Contribution: E.G., A.T., and F.H. designed the experiments, performed the research, and the analyzed data; E.G. and A.T. wrote the manuscript; A.A. prepared the clinical samples and performed the research; and A.T., H.K., and T.N. interpreted the data and supervised the experiments.

Conflict-of-interest disclosure: H.K. is a consultant for Kyowa Hakko Kogyo Co Ltd. The remaining authors declare no competing financial interests.

Correspondence: Akihiro Tomita, Department of Hematology and Oncology, Nagoya University Graduate School of Medicine, Tsurumai-cho 65, Showa-ku, Nagoya 466-8550, Japan; e-mail: atomita@med.nagoya-u.ac.jp.

References

1. Kakizuka A, Miller WH Jr, Umesono K, et al. Chromosomal translocation t(15;17) in human acute promyelocytic leukemia fuses RAR alpha with a novel putative transcription factor, PML. *Cell.* 1991;66(4):663-674.
2. Huang ME, Ye YC, Chen SR, et al. Use of all-trans retinoic acid in the treatment of acute promyelocytic leukemia. *Blood.* 1988;72(2):567-572.
3. Ohno R, Yoshida H, Fukutani H, et al. Multi-institutional study of all-trans-retinoic acid as a differentiation therapy of refractory acute promyelocytic leukemia. Leukaemia Study Group of the Ministry of Health and Welfare. *Leukemia.* 1993;7(11):1722-1727.
4. Kanamaru A, Takemoto Y, Tanimoto M, et al. All-trans retinoic acid for the treatment of newly diagnosed acute promyelocytic leukemia. Japan Adult Leukemia Study Group. *Blood.* 1995;85(5): 1202-1206.
5. Lo-Coco F, Avvisati G, Vignetti M, et al. Front-line treatment of acute promyelocytic leukemia with AIDA induction followed by risk-adapted consolidation for adults younger than 61 years: results of the AIDA-2000 trial of the GIMEMA Group. *Blood.* 2010;116(17):3171-3179.
6. Sanz MA, Montesinos P, Vellenga E, et al. Risk-adapted treatment of acute promyelocytic leukemia with all-trans retinoic acid and anthracycline monochemotherapy: long-term outcome of the LPA 99 multicenter study by the PETHEMA Group. *Blood.* 2008;112(8):3130-3134.
7. Asou N, Kishimoto Y, Kiyoi H, et al. A randomized study with or without intensified maintenance chemotherapy in patients with acute promyelocytic leukemia who have become negative for PML-RARalpha transcript after consolidation therapy: the Japan Adult Leukemia Study Group (JALSG) APL97 study. *Blood.* 2007;110(1):59-66.
8. Niu C, Yan H, Yu T, et al. Studies on treatment of acute promyelocytic leukemia with arsenic trioxide: remission induction, follow-up, and molecular monitoring in 11 newly diagnosed and 47 relapsed acute promyelocytic leukemia patients. *Blood.* 1999;94(10):3315-3324.
9. Wang ZY, Chen Z. Acute promyelocytic leukemia: from highly fatal to highly curable. *Blood.* 2008; 111(5):2505-2515.
10. Shen ZX, Chen GQ, Ni JH, et al. Use of arsenic trioxide (As2O3) in the treatment of acute promyelocytic leukemia (APL): II. Clinical efficacy and pharmacokinetics in relapsed patients. *Blood.* 1997;89(9):3354-3360.
11. Soignet SL, Frankel SR, Douer D, et al. United States multicenter study of arsenic trioxide in relapsed acute promyelocytic leukemia. *J Clin Oncol.* 2001;19(18):3852-3860.
12. Powell BL, Moser B, Stock W, et al. Arsenic trioxide improves event-free and overall survival for adults with acute promyelocytic leukemia: North American Leukemia Intergroup Study C9710. *Blood.* 2010;116(19):3751-3757.
13. Emadi A, Gore SD. Arsenic trioxide - An old drug rediscovered. *Blood Rev.* 2010;24(4-5):191-199.
14. Zhu J, Koken MH, Quignon F, et al. Arsenic-induced PML targeting onto nuclear bodies: implications for the treatment of acute promyelocytic leukemia. *Proc Natl Acad Sci U S A.* 1997;94(8): 3978-3983.
15. Müller S, Matunis MJ, Dejean A. Conjugation with the ubiquitin-related modifier SUMO-1 regulates the partitioning of PML within the nucleus. *EMBO J.* 1998;17(1):61-70.
16. Lallemand-Breitenbach V, Zhu J, Puvion F, et al. Role of promyelocytic leukemia (PML) sumolation in nuclear body formation, 11S proteasome recruitment, and As2O3-induced PML or PML/retinoic acid receptor alpha degradation. *J Exp Med.* 2001;193(12):1361-1371.
17. Tatham MH, Geoffroy MC, Shen L, et al. RNF4 is a poly-SUMO-specific E3 ubiquitin ligase required for arsenic-induced PML degradation. *Nat Cell Biol.* 2008;10(5):538-546.
18. Sun Y, Kim SH, Zhou DC, et al. Acute promyelocytic leukemia cell line AP-1060 established as a cytokine-dependent culture from a patient clinically resistant to all-trans retinoic acid and arsenic trioxide. *Leukemia.* 2004;18(7):1258-1269.
19. Dai J, Weinberg RS, Waxman S, Jing Y. Malignant cells can be sensitized to undergo growth inhibition and apoptosis by arsenic trioxide through modulation of the glutathione redox system. *Blood.* 1999;93(1):268-277.
20. Davison K, Cote S, Mader S, Miller WH. Glutathione depletion overcomes resistance to arsenic trioxide in arsenic-resistant cell lines. *Leukemia.* 2003;17(5):931-940.
21. Kitamura K, Minami Y, Yamamoto K, et al. Involvement of CD95-independent caspase 8 activation in arsenic trioxide-induced apoptosis. *Leukemia.* 2000;14(10):1743-1750.
22. Borden KL, Campbell Dwyer EJ, Salvato MS. An arenavirus RING (zinc-binding) protein binds the oncoprotein promyelocyte leukemia protein (PML) and relocates PML nuclear bodies to the cytoplasm. *J Virol.* 1998;72(1):758-766.
23. Saurin AJ, Borden KL, Boddy MN, Freemont PS. Does this have a familiar RING? *Trends Biochem Sci.* 1996;21(6):208-214.
24. Zhang XW, Yan XJ, Zhou ZR, et al. Arsenic trioxide controls the fate of the PML-RARalpha oncoprotein by directly binding PML. *Science.* 2010;328(5975):240-243.
25. Jeanne M, Lallemand-Breitenbach V, Ferhi O, et al. PML/RARA oxidation and arsenic binding initiate the antileukemia response of As2O3. *Cancer Cell.* 2010;18(1):88-98.
26. Atsumi A, Tomita A, Kiyoi H, Naoe T. Histone deacetylase 3 (HDAC3) is recruited to target promoters by PML-RARalpha as a component of the N-CoR co-repressor complex to repress transcription in vivo. *Biochem Biophys Res Commun.* 2006;345(4):1471-1480.
27. Hiraga J, Tomita A, Sugimoto T, et al. Down-regulation of CD20 expression in B-cell lymphoma cells after treatment with rituximab-containing combination chemotherapies: its prevalence and clinical significance. *Blood.* 2009; 113(20):4885-4893.
28. Tomita A, Buchholz DR, Obata K, Shi YB. Fusion protein of retinoic acid receptor alpha with promyelocytic leukemia protein or promyelocytic leukemia zinc finger protein recruits N-CoR-TBLR1 corepressor complex to repress transcription in vivo. *J Biol Chem.* 2003;278(33):30788-30795.
29. Tomita A, Buchholz DR, Shi YB. Recruitment of N-CoR/SMRT-TBLR1 corepressor complex by unliganded thyroid hormone receptor for gene repression during frog development. *Mol Cell Biol.* 2004;24(8):3337-3346.
30. Hayakawa F, Privalsky ML. Phosphorylation of PML by mitogen-activated protein kinases plays a key role in arsenic trioxide-mediated apoptosis. *Cancer Cell.* 2004;5(4):389-401.
31. Golomb HM, Rowley JD, Vardiman JW, Testa JR, Butler A. "Microgranular" acute promyelocytic leukemia: a distinct clinical, ultrastructural, and cytogenetic entity. *Blood.* 1980;55(2):253-259.
32. Pandolfi PP, Alcalay M, Fagioli M, et al. Genomic variability and alternative splicing generate multiple PML/RAR alpha transcripts that encode aberrant PML proteins and PML/RAR alpha isoforms in acute promyelocytic leukaemia. *EMBO J.* 1992;11(4):1397-1407.
33. Lallemand-Breitenbach V, Jeanne M, Benhenda S, et al. Arsenic degrades PML or PML-RARalpha through a SUMO-triggered RNF4/ubiquitin-mediated pathway. *Nat Cell Biol.* 2008;10(5): 547-555.
34. Borden KL, Lally JM, Martin SR, O'Reilly NJ, Solomon E, Freemont PS. In vivo and in vitro characterization of the B1 and B2 zinc-binding domains from the acute promyelocytic leukemia protooncoprotein PML. *Proc Natl Acad Sci U S A.* 1996;93(4):1601-1606.
35. Flenghi L, Fagioli M, Tomassoni L, et al. Characterization of a new monoclonal antibody (PG-M3) directed against the aminoterminal portion of the PML gene product: immunocytochemical evidence for high expression of PML proteins on activated macrophages, endothelial cells, and epithelia. *Blood.* 1995;85(7):1871-1880.
36. Fagioli M, Alcalay M, Tomassoni L, et al. Cooperation between the RING + B1-B2 and coiled-coil domains of PML is necessary for its effects

on cell survival. *Oncogene.* 1998;16(22):2905-2913.

37. Huang W, Sun GL, Li XS, et al. Acute promyelocytic leukemia: clinical relevance of two major PML-RAR alpha isoforms and detection of minimal residual disease by retrotranscriptase/polymerase chain reaction to predict relapse. *Blood.* 1993;82(4):1264-1269.
38. Vahdat L, Maslak P, Miller WH Jr, et al. Early mortality and the retinoic acid syndrome in acute promyelocytic leukemia: impact of leukocytosis, low-dose chemotherapy, PMN/RAR-alpha isoform, and CD13 expression in patients treated with all-trans retinoic acid. *Blood.* 1994;84(11):3843-3849.
39. Ishov AM, Sotnikov AG, Negorev D, et al. PML is critical for ND10 formation and recruits the PML-interacting protein daxx to this nuclear structure when modified by SUMO-1. *J Cell Biol.* 1999;147(2):221-234.
40. Lallemand-Breitenbach V, de The H. PML nuclear bodies. *Cold Spring Harb Perspect Biol.* 2010;2(5):a000661.
41. Zhou DC, Kim SH, Ding W, Schultz C, Warrell RP Jr, Gallagher RE. Frequent mutations in the ligand-binding domain of PML-RARalpha after multiple relapses of acute promyelocytic leukemia: analysis for functional relationship to response to all-trans retinoic acid and histone deacetylase inhibitors in vitro and in vivo. *Blood.* 2002;99(4):1356-1363.
42. Côté S, Zhou D, Bianchini A, Nervi C, Gallagher RE, Miller WH Jr. Altered ligand binding and transcriptional regulation by mutations in the PML/RARalpha ligand-binding domain arising in retinoic acid-resistant patients with acute promyelocytic leukemia. *Blood.* 2000;96(9):3200-3208.
43. Ding W, Li YP, Nobile LM, et al. Leukemic cellular retinoic acid resistance and missense mutations in the PML-RARalpha fusion gene after relapse of acute promyelocytic leukemia from treatment with all-trans retinoic acid and intensive chemotherapy. *Blood.* 1998;92(4):1172-1183.
44. Imaizumi M, Suzuki H, Yoshinari M, et al. Mutations in the E-domain of RAR portion of the PML/RAR chimeric gene may confer clinical resistance to all-trans retinoic acid in acute promyelocytic leukemia. *Blood.* 1998;92(2):374-382.
45. Marasca R, Zucchini P, Galimberti S, et al. Missense mutations in the PML/RARalpha ligand binding domain in ATRA-resistant As(2)O(3) sensitive relapsed acute promyelocytic leukemia. *Haematologica.* 1999;84(11):963-968.
46. Lin RJ, Nagy L, Inoue S, Shao W, Miller WH Jr, Evans RM. Role of the histone deacetylase complex in acute promyelocytic leukaemia. *Nature.* 1998;391(6669):811-814.
47. Grignani F, De Matteis S, Nervi C, et al. Fusion proteins of the retinoic acid receptor-alpha recruit histone deacetylase in promyelocytic leukaemia. *Nature.* 1998;391(6669):815-818.
48. Zhu Q, Zhang JW, Zhu HQ, et al. Synergic effects of arsenic trioxide and cAMP during acute promyelocytic leukemia cell maturation subtends a novel signaling cross-talk. *Blood.* 2002;99(3):1014-1022.
49. Zhou J, Zhang Y, Li J, et al. Single-agent arsenic trioxide in the treatment of children with newly diagnosed acute promyelocytic leukemia. *Blood.* 2010;115(9):1697-1702.

Clin Exp Metastasis (2012) 29:207–216
DOI 10.1007/s10585-011-9443-3

RESEARCH PAPER

Erlotinib prevents experimental metastases of human small cell lung cancer cells with no epidermal growth factor receptor expression

Adel Gomaa Mohammed Gabr · Hisatsugu Goto · Masaki Hanibuchi · Hirohisa Ogawa · Takuya Kuramoto · Minako Suzuki · Atsuro Saijo · Soji Kakiuchi · Van The Trung · Satoshi Sakaguchi · Yoichiro Moriya · Saburo Sone · Yasuhiko Nishioka

Received: 2 September 2011 / Accepted: 6 December 2011 / Published online: 15 December 2011

Abstract Epidermal growth factor receptor–tyrosine kinase inhibitors (EGFR–TKIs) show dramatic antitumor activity in a subset of patients with non-small cell lung cancer who have an active mutation in the epidermal growth factor receptor (EGFR) gene. On the other hand, some lung cancer patients with wild type EGFR also respond to EGFR–TKIs, suggesting that EGFR–TKIs have an effect on host cells as well as tumor cells. However, the effect of EGFR–TKIs on host microenvironments is largely unknown. A multiple organ metastasis model was previously established in natural killer cell-depleted severe combined immunodeficient mice using human lung cancer cells. This model was used to investigate the therapeutic efficacy of erlotinib, an EGFR–TKI, on multiple organ metastases induced by human small cell lung cancer cells (SBC-5 cells) that did not express EGFR. Although erlotinib did not have any effect on the proliferation of SBC-5 cells in vitro, it significantly suppressed bone and lung metastases in vivo, but not liver metastases. An immunohistochemical analysis revealed that, erlotinib significantly suppressed the number of osteoclasts in bone metastases, whereas no difference was seen in microvessel density. Moreover, erlotinib inhibited EGF-induced receptor activator of nuclear factor kappa-B expression in an osteoblastic cell line (MC3T3-E1 cells). These results strongly suggested that erlotinib prevented bone metastases by affecting host microenvironments irrespective of its direct effect on tumor cells.

Keywords Erlotinib · Bone metastasis · Lung cancer · Host microenvironment

A. G. M. Gabr · T. Kuramoto · S. Kakiuchi · V. T. Trung · S. Sone
Department of Medical Oncology, Institute of Health Biosciences, The University of Tokushima Gradate School, Tokushima, Japan

H. Goto · M. Hanibuchi · M. Suzuki · A. Saijo · S. Sakaguchi · S. Sone · Y. Nishioka (✉)
Department of Respiratory Medicine and Rheumatology, Institute of Health Biosciences, The University of Tokushima Graduate School, 3-18-15 Kuramoto-cho, Tokushima 770-8503, Japan
e-mail: yasuhiko@clin.med.tokushima-u.ac.jp

H. Ogawa
Department of Molecular and Environmental Pathology, Institute of Health Biosciences, The University of Tokushima Gradate School, Tokushima, Japan

Y. Moriya
Chugai Pharmaceutical Co., Ltd., Tokyo, Japan

Abbreviations

EGFR–TKI	Epidermal growth factor receptor–tyrosine kinase inhibitor
NSCLC	Non-small cell lung cancer
NK	Natural killer
SCID	Severe combined immunodeficient
SCLC	Small cell lung cancer
PTHrP	Parathyroid hormone-related protein
EGFR	Epidermal growth factor receptor
HUVECs	Human umbilical vein endothelial cells
IL	Interleukin
Ab	Antibody
VEGF	Vascular endothelial growth factor
MTT	3-(4,5-Dimethylthiazol-2-yl)-2,5-diphenyl tetrazolium
BMMSCs	Bone marrow mesenchymal stem cells
HGF	Hepatocyte growth factor

Introduction

Lung cancer is the major cause of malignancy-related death worldwide. The mortality rate is 80–90%, which makes this disease the leading cause of cancer-related death [1]. The high mortality of this disease is primarily due to the difficulty of early diagnosis and the highly metastatic potential. Approximately 70% of lung cancer patients have already developed metastases to multiple organs by the time of the diagnosis [2]. There is no curative therapy for the metastases, and clinical management is palliative in many cases. Therefore, it is crucial to prevent and treat lung cancer metastases.

Although the outcome of conventional chemotherapy for patients with advanced lung cancer is still unsatisfactory, recent studies have enabled the development of molecular targeting agents such as epidermal growth factor receptor–tyrosine kinase inhibitors (EGFR–TKIs). Treatment with the reversible EGFR–TKIs (gefitinib and erlotinib) results in dramatic antitumor activity in a subset of patients with non-small cell lung cancer (NSCLC). Approximately 75% of patients with epidermal growth factor receptor (EGFR) mutations respond to EGFR–TKIs [3, 4]. The inhibition of EGFR tyrosine kinase results in the induction of substantial apoptosis in these tumor cells because lung cancer cells that have an active mutation in the EGFR gene become addicted to the EGFR signaling pathway for their growth. This mechanism allows EGFR–TKIs to exert anti-tumor activity in NSCLC patients with an active mutation in the EGFR gene.

However, it is noteworthy that an objective response of about 10% is also achieved with erlotinib treatment in NSCLC patients with wild type EGFR [5]. These clinical observations indicate that EGFR–TKIs might have other mechanisms of action in addition to their direct effect on tumor cells. Normanno et al. [6] demonstrated that gefitinib inhibits the recruitment of osteoclasts in bone lesions, by affecting the ability of bone marrow stromal cells to induce osteoclast differentiation and activation. Moreover, Cerniglia et al. [7] reported that erlotinib treatment of tumor-bearing mice alters vessel morphology and decreases vessel permeability in tumor xenografts. These observations suggest that EGFR–TKIs have the potential to modulate and affect host cells, but their effect on the host microenvironment in different organs with cancer metastases is largely unknown.

The establishment of clinically relevant experimental metastasis models is crucial to understand the pathogenesis of lung cancer and its relationship to host microenvironment. A reproducible model of multiple organ metastases by human lung cancer cells was previously established in natural killer (NK) cell-depleted severe combined immunodeficient (SCID) mice [8, 9]. This model was used to elucidate the mechanisms of interactions of metastatic lung cancer cells with host organ microenvironment and the heterogeneity in organ microenvironments on the metastases of human lung cancer [10–14].

The present study sought to elucidate the action of EGFR–TKIs on host microenvironments in organs with lung cancer metastases. The study investigated the therapeutic efficacy of erlotinib, an EGFR–TKI, on multiple organ metastases induced by SBC-5 human small cell lung cancer (SCLC) cells that did not express EGFR in NK cell-depleted SCID mice.

Materials and methods

Cell cultures

The human SCLC cell line, SBC-5 [15] was kindly provided by Drs. M. Tanimoto and K. Kiura (Okayama University, Okayama, Japan). The PC-9 human adenocarcinoma cell line was purchased from the American Type Culture Collection (Manassas, VA). SBC-5 cells were maintained in Eagle's MEM (Nissui Pharmaceutical Co., Tokyo, Japan) supplemented with 10% heat-inactivated fetal bovine serum (FBS, GIBCO, Grand Island, NY), penicillin (100 U/ml), and streptomycin (50 μg/ml). PC-9 cells were maintained in RPMI1640 (Nissui Pharmaceutical Co., Tokyo, Japan) supplemented with 10% heat-inactivated FBS, penicillin and streptomycin. The MC3T3-E1 murine osteoblastic cell line subclone 4 was kindly provided by Chugai Pharmaceutical Co., Ltd. (Tokyo, Japan). MC3T3-E1 cells were maintained as preosteoblasts in α-MEM growth medium supplemented with 10% FBS, penicillin and streptomycin. The growth medium was supplemented with L-ascorbic acid (50 μg/ml) to induce differentiation, and the cells were cultured for 7 days [16]. All cell lines were incubated at 37°C in a humidified atmosphere of 5% CO_2 in air.

Reagents

An anti-mouse interleukin (IL)-2 receptor β chain monoclonal antibody (Ab), TM-β1 (IgG2b), was kindly provided by Drs. M. Miyasaka and T. Tanaka (Osaka University, Osaka, Japan) [17]. Recombinant murine EGF was purchased from Invitrogen (Carlsbad, CA). None of these materials contained endotoxins, as determined by the limulus amebocyte assay (Seikagaku Kogyo, Tokyo, Japan: minimum detection level, 0.1 ng/ml).

In vitro cell proliferation and migration assay

Cell proliferation was determined using the 3-(4,5-dimethylthiazol-2-yl)-2,5-diphenyl tetrazolium (MTT) dye reduction method [18]. The human lung cancer cells

(2×10^3 cells/100 μl) were plated into each well of a 96-well plate, and incubated overnight. Various concentrations of erlotinib were added and the cells incubated for 72 h. Fifty microliters of stock MTT solution (2 mg/ml; Sigma-Aldrich, St. Louis, MO) was added to all wells, and the cells were then further incubated for 2 h at 37°C. The media containing MTT solution were removed, and 100 μl of DMSO (Sigma-Aldrich, St. Louis, MO) was added. The absorbance was measured with an MTP-32 Microplate Reader (Corona Electric, Ibaragi, Japan) at test and reference wavelengths of 550 and 630 nm, respectively. Cell migration was determined using double chamber method. RPMI-1640 medium (0.75 ml) containing 10% FBS was applied to the lower chamber as chemoattractant, and SBC-5 cells (5×10^4) in 0.5 ml of serum-free RPMI-1640 medium were seeded in inner chamber (8 μm-pore, BD Labware, Franklin Lakes, NJ) with the presence of 0, 0.01, 0.1 or 1 μM erlotinib, and incubated for 19 h at 37°C. After incubation, cells remaining on the upper side of the insert were removed, and the cells that migrated to the lower surface of the insert were counted in four different random fields at 100× magnification. Each treatment was performed in triplicate.

Animals

Male, 6 to 8-week-old S EB-17/Icr-scid mice were obtained from Clea Japan (Osaka, Japan) and maintained under specific pathogen-free conditions throughout the experiment. The experimental protocol was reviewed and approved by the animal care and use committee of The University of Tokushima, and were performed according to their guidelines.

Experimental metastasis with SBC-5 cells and the effect of erlotinib

NK cells were depleted in SCID mice to facilitate the metastasis of human lung cancer cell lines. TM-β1 Ab (0.3 mg/mouse) was injected i.p. into SCID mice 2 days before tumor inoculation [8]. Tumor cells were harvested and washed with Ca^{2+}- and Mg^{2+}-free phosphate buffered saline (Nissui Pharmaceutical Co., Tokyo, Japan). Cell viability was determined by a trypan blue exclusion test and only single cell suspensions of >90% viability were used. SBC-5 cells (1×10^6 cells/0.3 ml/mouse) were inoculated into the lateral tail vein of unanesthetized SCID mice pretreated with TM-β1 Ab on day 0. Oral administration of erlotinib (10 or 30 mg/kg) was performed once daily from day 7 to 28. Vehicle was administered to the control group. Mice were anesthetized and humanely sacrificed on day 29 by cutting the subclavian artery, and all major organs were removed. Whole body X-ray photographs (Fuji Film, Tokyo, Japan) of tumor-bearing mice were taken just before sacrifice and bone metastases were independently evaluated on X-ray photographs by two authors [9]. The lungs were fixed in Bouin's solution (Sigma-Aldrich, St. Louis, MO) for 24 h. The number of metastatic foci on the lungs, liver were counted macroscopically.

Immunohistochemistry

The hind limbs of the mice were taken and fixed in 10% formalin. The bone specimens were decalcified in 10% EDTA solution for 1 week and then embedded in paraffin. The paraffin-embedded tissue samples were cut into 3-μm sections and picked up on slides. Tartrate-resistant acid phosphatase (TRAP) staining was performed using a Sigma Diagnostics Acid Phosphatase Kit (Sigma Diagnostics, St. Louis, MO) for the detection of osteoclasts. The number of TRAP-positive osteoclasts at the tumor-bone interface in each slide was counted under a microscope in five random fields at 200× magnification. Formalin fixed, paraffin embedded sections were stained with anti-mouse CD31 Ab (Santa Cruz Biotechnology, Santa Cruz, CA). CD31 positive microvessels were counted from five independent fields at 200× magnification of each section. The sections were also stained with H&E for routine histologic examination.

Western blot analysis

The cells were seeded at 1×10^6 cells/dish in corresponding differentiation conditions to assess the effects of exogenous stimuli on the activation of the EGFR in MC3T3-E1 cells. Differentiated cells were cultured for 24 h in medium containing 1% FBS, and subsequently treated with recombinant EGF for 10 min in the absence or presence of various concentrations of erlotinib. Cells were lysed in M-PER (Pierce, Rockford, IL) containing phosphatase inhibitor cocktail and proteinase inhibitor cocktail (Roche Diagnostics, Indianapolis, IN), and the protein concentration was determined using a protein assay kit (Bio-Rad, Hercules, CA). Aliquots of 400 μg of total protein were immunoprecipitated with the anti-mouse EGFR Ab (Cell signaling, Danvers, MA), and the immune complexes were recovered with Protein G-Sepharose beads (GE Healthcare, Buckinghamshire, UK). Proteins were separated by SDS-PAGE (Invitrogen, Carlsbad CA) and then transferred to PVDF membranes (Atto, Tokyo, Japan). Washed membranes were incubated with Blocking One (Nacalai Tesque, Kyoto, Japan) for 1 h at room temperature, then incubated 1 h at room temperature with anti-phosphotyrosine Ab (1:1,000 dilution, cell signaling) or anti-EGFR Ab (1:2,00 dilution, cell signaling). The membranes were

incubated for 30 min at room temperature with species-specific horseradish peroxidase conjugated secondary antibodies, and the immunoreactive bands were visualized using an enhanced chemiluminescent substrate (Pierce, Rockford, IL).

Reverse transcription polymerase chain reaction

MC3T3-E1 cells were seeded at 1×10^6 cells/well in 6-well plates in the corresponding differentiation conditions. The differentiated cells were treated with recombinant EGF in the absence or presence of indicated dose of erlotinib for 48 h. Total cellular RNA was isolated by using RNeasy Mini kit (Qiagen, Valencia, CA) according to the manufacturer's protocols. RNA (0.5–2.0 μg) was reverse transcribed using a TaqMan® RNA-to-CT™ 2-Step kit (Applied biosystems, Foster City, CA). Messenger The expression of receptor activator of nuclear factor kappa-B ligand (RANKL), osteoprotegerin (OPG) and EGFR mRNA were measured by real-time polymerase chain reaction (PCR) using Assay on Demand Taqman Gene expression primers and probes (Applied biosystems). PCR reaction conditions were those recommended by the manufacturer. Fluorescence signals were monitored after each PCR cycle with an ABI Prism 7700 sequence detection system (Applied Biosystems). C_T values (cycle number where fluorescence exceeded a fixed threshold) were obtained for each target probe and normalized with the corresponding C_T values for the internal control (mouse $\beta 2$ microglobulin). The RNA levels were expressed as relative units.

Statistical analysis

The Mann–Whitney *U* test was used to evaluate the differences in the numbers of metastases into multiple organs (bone, liver, and lung) between the erlotinib-treated groups and the control (vehicle treated group), and to evaluate the differences in immunohistochemistry. The differences in in vitro experiments were analyzed by Student's *t* test (two-tailed). A *P* value of <0.05 was considered to be significant in all experiments.

Results

Erlotinib did not affect the proliferation and migration of human SCLC, SBC-5 cells in vitro

We have previously reported that SBC-5 cells do not express EGFR [12]. In this study, we first examined the effect of erlotinib on in vitro proliferation and migration of SBC-5 cells. As shown in Fig. 1a, clinically relevant doses

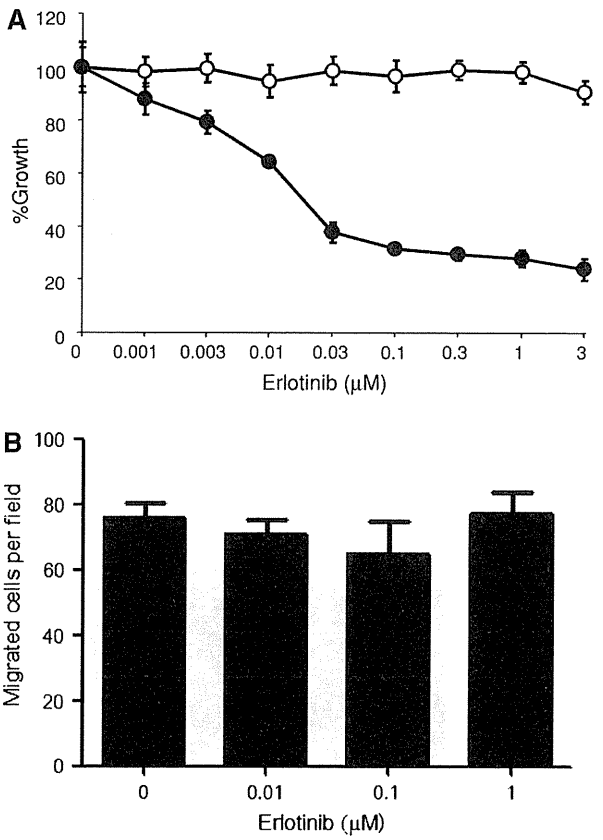

Fig. 1 Effect of erlotinib on the proliferation and migration of human SCLC, SBC-5 cells in vitro. **a** SBC-5 cells (1×10^3 cells/well; *open circles*) or PC-9 cells (1×10^3 cells/well; *closed circles*) were plated into each well of a 96-well plate and incubated overnight. Various concentrations of erlotinib were added and the cells were incubated for 72 h. Cell growth was determined by MTT assay as described in "Materials and methods" section. *Bars* show SDs of the means of triplicate cultures. Data are representative of five independent experiments. **b** Cell migration of SBC-5 cells was assessed as described in "Materials and methods" section. *Bars* show SDs of the means of triplicate cultures. Data are representative of two independent experiments

(3 μM or less) of erlotinib [19] had no effect on the proliferation of SBC-5 cells. On the contrary, erlotinib significantly inhibited the proliferation of PC-9 cells, which harbor a deletion mutation on exon 19 of the EGFR gene, in a dose-dependent fashion (Fig. 1a), consistent with a previous report [20]. Cell migration of SBC-5 cells was also not affected by erlotinib treatment (Fig. 1b).

Treatment with erlotinib inhibited bone and lung metastases by SBC-5 cells in NK cell-depleted SCID mice

A multiple organ metastasis model with SBC-5 cells was established in SCID mice depleted of NK cells [9]. Intravenously inoculated SBC-5 cells (1×10^6/mouse)

developed metastatic colonies in the lungs, liver, and bones (osteolytic metastasis) of NK cell-depleted SCID mice. This model was used to assess the therapeutic efficacy of erlotinib. Oral administration of erlotinib (30 mg/kg) from day 7 to 28 significantly inhibited the formation of osteolytic bone metastases (Fig. 2). Interestingly, treatment with erlotinib also inhibited distant metastases in the lungs, although it had no effect on liver metastases (Table 1). Erlotinib treatment was well tolerated and no obvious adverse events, such as body weight loss, were observed even in the 30 mg/kg group (data not shown). These in vivo results suggested that erlotinib prevented distant metastases by affecting the host microenvironments because erlotinib had no direct effect on the proliferation of SBC-5 cells in vitro.

Effect of erlotinib on tumor angiogenesis

Guillamo et al. [21] reported that EGFR–TKI (gefitinib) inhibits angiogenesis in a mouse experimental glioma model. Moreover, Riedel et al. [22] reported that addition of conditioned medium from EGFR antisense-treated tumor cells decreases endothelial cell migration and proliferation. These findings suggested that the prevention of SBC-5-induced metastasis formation by erlotinib could be due to the inhibition of angiogenesis. However, immunohistochemical staining with CD31 revealed no significant difference in the microvessel density in the lung, bone, and liver (Fig. 3). The effect of erlotinib on the proliferation of human umbilical vein endothelial cells (HUVECs) was also evaluated in vitro. Up to 3 μM of erlotinib did not

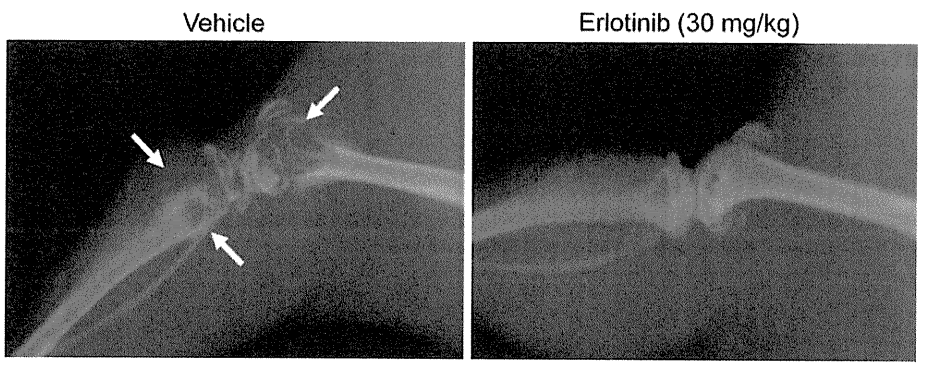

Fig. 2 Therapeutic efficacy of erlotinib against osteolytic bone metastases produced by human SCLC, SBC-5 cells. SBC-5 cells (1×10^6 cells/mouse) were inoculated into the tail vein of NK cell-depleted SCID mice. Oral administration of erlotinib was performed as described in "Materials and methods" section. Mice were sacrificed and bone metastases were determined radiographically on day 29. The representative pictures of vehicle- and erlotinib-treated mice are shown. The *arrows* indicate osteolytic bone metastases

Table 1 Effect of erlotinib on multiple organ metastasis produced by SBC-5 cells

Treatment	Bone			Liver					Lung				
	Number of metastasis			Weight (g)		Number of metastasis			Weight (g)		Number of metastasis		
	Inc.	Med.	Range	Med.	Range	Inc.	Med.	Range	Med.	Range	Inc.	Med.	Range
Experiment 1													
Vehicle	6/6	6	5–7	1.6	1.3–1.9	6/6	39	25–80	0.3	0.3–0.4	6/6	38	30–55
10 mg/kg	5/5	5	3–6	1.4	1.0–1.7	5/5	23	12–35	0.3	0.2–0.5	5/5	20	8–30
30 mg/kg	5/5	3*	2–5	2.0	1.8–3.4	5/5	26	2–38	0.3	0.3–0.4	5/5	15*	6–35
Experiment 2													
Vehicle	6/6	9	7–11	1.8	1.6–2.4	6/6	60	20–150	0.22	0.24–0.41	6/6	14	5–20
10 mg/kg	6/6	8	5–11	1.6	1.3–1.8	6/6	31	10–50	0.24	0.29–0.4	6/6	10	9–11
30 mg/kg	6/6	4*	2–6	1.5	1.8–3.3	6/6	24	12–40	0.21	0.3–0.4	6/6	7*	2–11

SBC-5 cells (1×10^6 cells/mouse) were inoculated i.v. into NK cell-depleted SCID mice on day 0. Erlotinib (or vehicle) was given orally from day 7 to 28 after tumor cell inoculation. The metastatic profile was evaluated on day 29. Mann–Whitney *U* test was used to determine the significance of differences

Inc. incidence, *Med.* median

* Statistically significant difference compared with vehicle-treated group ($P < 0.05$)

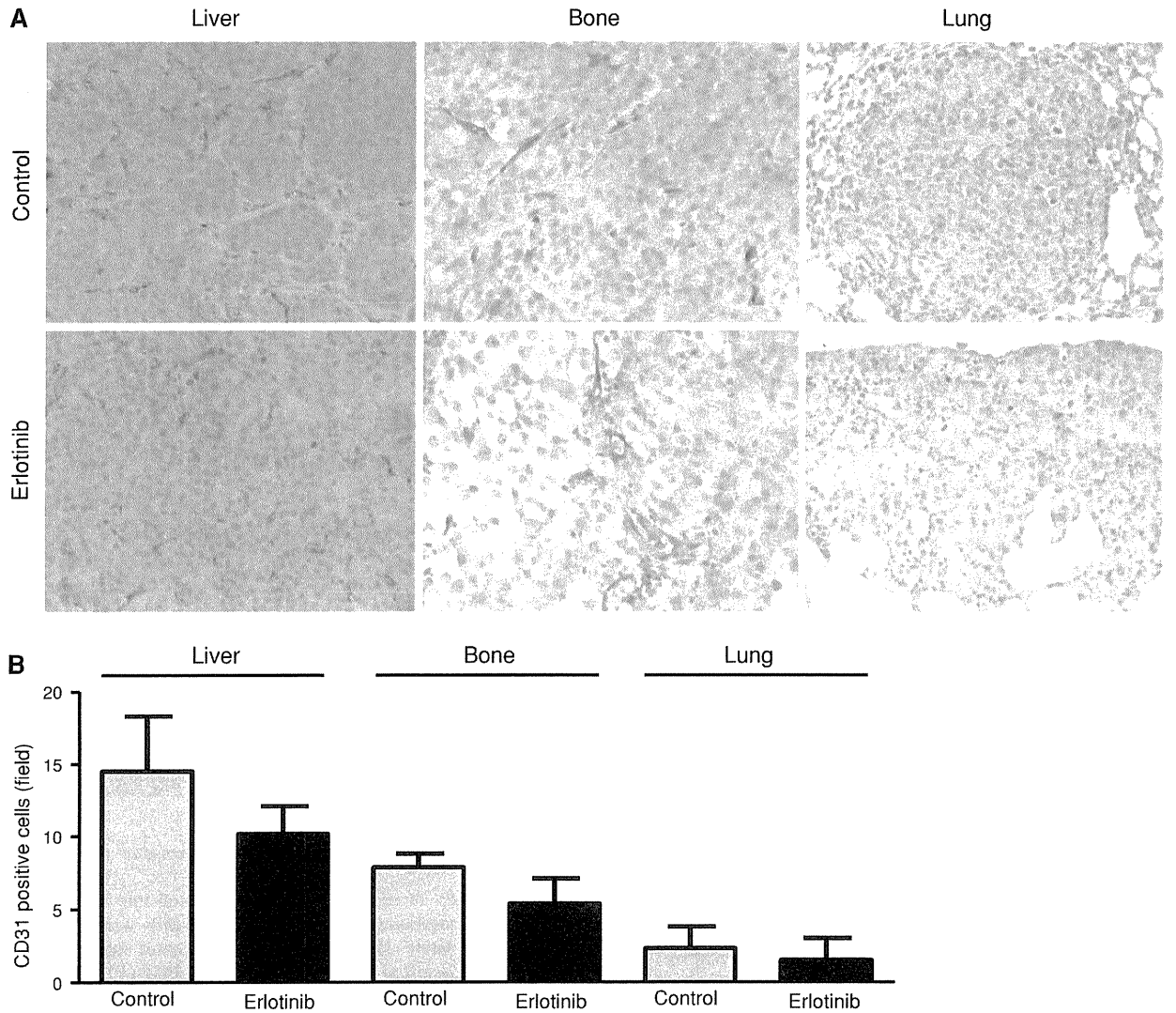

Fig. 3 Effect of erlotinib on tumor angiogenesis. SBC-5 cells (1×10^6 cells/mouse) were inoculated into the tail vein of NK cell-depleted SCID mice. Oral administration of erlotinib was performed as described in "Materials and methods" section. Each organ was collected on day 29, paraffin embedded, and sections were subjected to immunohistochemical staining of CD31. **a** Representative pictures of immunohistochemical staining are shown (magnification, ×200). **b** CD31 positive microvessels were counted from five independent fields of each section. *Bars* show SEM of the means for five mice per group

affect the proliferation of HUVECs irrespective of the stimulation with recombinant human vascular endothelial growth factor (VEGF) (data not shown).

Erlotinib reduced the number of osteoclast in bone metastasis lesion

A previous study demonstrated the importance of osteoclasts in bone metastasis development by SBC-5 cells [9, 10]. Immunohistochemical staining (TRAP staining) was performed to evaluate the number of osteoclasts in metastatic bone lesions. Figure 4 demonstrates that erlotinib treatment significantly reduced the number of osteoclasts (TRAP positive cells) in metastatic bone lesions.

Erlotinib inhibited EGF-induced RANKL expression in osteoblastic cell line MC3T3-E1 cells

RANKL is one of the key molecules responsible for the formation of osteolytic bone metastasis in various types of cancer [23]. RANKL expressed by osteoblasts activates osteoclasts by binding to its receptor (RANK). The fact that the number of osteoclasts in bone metastasis lesions decreased after erlotinib treatment suggested that erlotinib

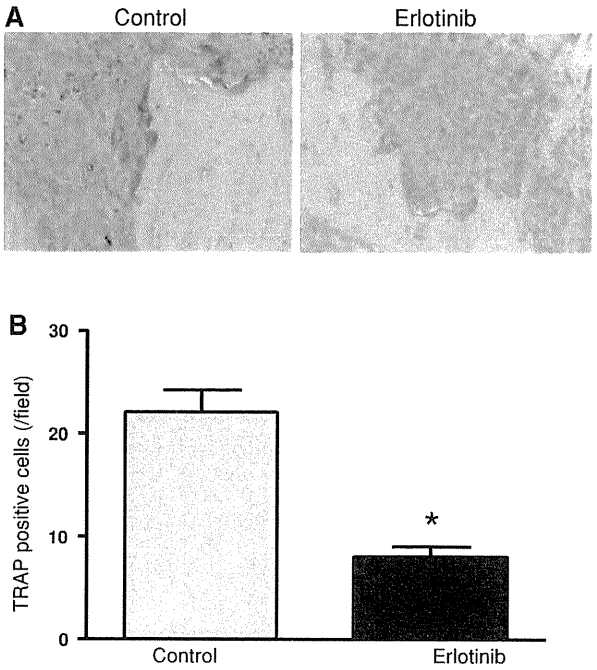

Fig. 4 The effect of erlotinib on osteoclast recruitment in metastatic bone lesion. SBC-5 cells (1×10^6 cells/mouse) were inoculated into the tail vein of NK cell-depleted SCID mice. Oral administration of erlotinib was performed as described in "Materials and methods" section. Metastatic bone lesions were collected on day 29, and sections were subjected to TRAP staining to evaluate osteoclast recruitment. **a** Representative pictures of TRAP staining of bone are shown (magnification, ×200). TRAP positive cells were stained in *purple*. **b** The number of osteoclasts (TRAP positive cells) was counted from five independent fields of each section. *Bars* show the SEM of the means for five mice per group. $^*P < 0.01$

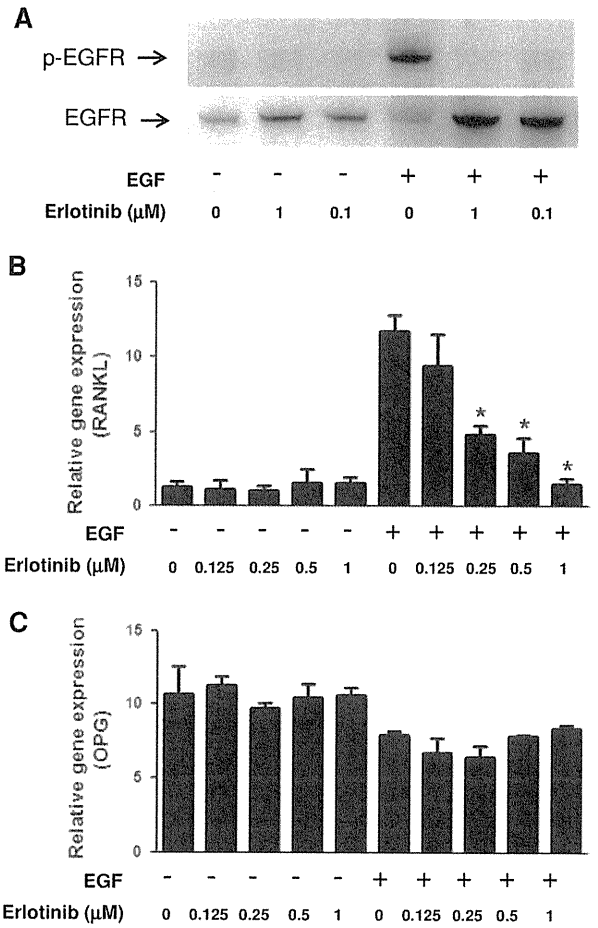

Fig. 5 The effect of erlotinib on osteoblastic cell line MC3T3-E1 cells. Murine osteoblastic cell line MC3T3-E1 cells were differentiated into the mature state as described in "Materials and methods" section. **a** Differentiated cells were treated with EGF (10 ng/ml) for 10 min in the presence or absence of erlotinib. Expression of EGFR and phosphorylated EGFR (p-EGFR) was detected by western blotting. **b**, **c** Differentiated MC3T3-E1 cells were treated with EGF (10 ng/ml) in the presence or absence of various concentrations of erlotinib for 48 h. The cells were harvested, and the expression of **b** RANKL and **c** OPG was detected by RT-PCR. *Bars* show the SEM of the means of triplicate cultures. $^*P < 0.01$

suppresses osteoclast differentiation and activation by inhibiting the RANK–RANKL axis. The expression of EGFR in the osteoblastic cell line MC3T3-E1 cells was evaluated, since EGFR is reported to be expressed in osteoblasts but not in osteoclasts [16]. Figure 5a shows that MC3T3-E1 cells did express EGFR, and its phosphorylation was induced by EGF treatment. The inhibition of EGFR phosphorylation by erlotinib was also confirmed. EGF induced RANKL expression in MC3T3-E1 cells, and the expression was significantly suppressed by erlotinib in a dose dependent manner (Fig. 5b). Interestingly, the expression of OPG, the decoy receptor for RANKL, was not affected by either EGF or erlotinib treatment (Fig. 5c).

Discussion

The present study demonstrated that erlotinib significantly suppressed bone and lung metastases, but not liver metastases, by SBC-5 cells that did not express EGFR. These findings suggest the importance of the host microenvironment in the treatment of lung cancer with erlotinib. The formation of distant metastasis involves several sequential steps, including tumor growth in the primary site, invasion into blood vessels, arrest in the capillaries, extravasation, invasion and growth in target organs [24, 25]. Molecular interactions between cancer cells and their microenvironments play important roles that allow the cancer cells to survive at metastatic sites, [24–27]. Therefore, the efficacy of therapeutic agents against cancer metastases depends on their mechanisms of action on tumor cells as well as the host microenvironments.

There is accumulating evidence that the EGFR ligand-EGFR axis plays a role in in bone biology and pathology. The expression and functionality of EGFR has been clearly

demonstrated in bone marrow mesenchymal stem cells (BMMSCs) [6, 28], and osteoblasts themselves differentiate from mesenchymal stem cells [29]. In addition, EGFR ligands, such as EGF and amphiregulin, stimulate the proliferation of BMMSCs and osteoblasts [30–32], suggesting that EGFR ligands are mitogens for BMMSCs and osteoblasts. EGFR signaling also indirectly affects osteoclast formation, although osteoclasts do not express functional EGFR [16]. The role of EGFR in osteoclast formation suggests that the balance of RANKL and OPG (the decoy receptor for RANKL), which are expressed by osteoblasts, is associated with differentiation. The current study showed that the expression of RANKL, not OPG, in osteoblasts was stimulated by EGF, and this might enhance osteoclast activation via the RANK/RANKL axis. This result is supported by previous study reported by Furugaki et al. [33]. Using mouse osteolytic bone invasion model, they showed that the lung cancer cells induced RANKL expression of osteoblasts, and erlotinib inhibited the tumor-induced osteolytic invasion by suppressing osteoclast activation through inhibiting osteolytic factor production including RANKL. The importance of the balance of RANKL and OPG is also supported by Zhu et al. [16]. They demonstrated that EGFR ligands stimulate osteoclast formation by inhibiting the expression of OPG by osteoblasts, although RANKL expression was not affected. This difference might be due to differences in the experimental conditions and EGFR ligands. The importance of osteoclasts and osteoblasts on the development of bone metastases [16, 34] suggests that EGFR–TKIs prevent bone metastasis formation by inhibiting the activation of osteoclasts and osteoblasts in addition to their direct effect on tumor cells.

Current evidence also suggests the association of EGFR signaling with primary bone tumor and bone metastasis formation. EGFR upregulation is observed in osteosarcomas and osteosarcoma cell lines [35], bone and soft tissue tumors [36]. Furthermore, EGFR is overexpressed in a variety of tumors metastasizing to bone. Prostate cancer is the best studied example. EGFR expression correlates with prostate cancer relapse and progression to androgen independence [37] and the blockade of EGFR signaling by PKI166, an EGFR–TKI, inhibits prostate cancer growth in the bones of nude mice [38]. Gefitinib, an EGFR–TKI, inhibits the recruitment of osteoclasts in metastatic bone lesions from breast cancer by affecting the ability of bone marrow stromal cells to induce osteoclast differentiation and activation [6]. Moreover, gefitinib administered to breast cancer patients (phase II trial) with bone metastasis significantly attenuates and relieves bone pain [6]. Collectively, EGFR–TKIs might thus have the potential to regulate the progression of bone metastases by acting on not only tumor cells but also host microenvironments, thus suggesting the importance of targeting the EGFR signaling blockade in the prevention of bone metastases.

The current study found that erlotinib prevented distant metastases in the bone and the lungs but not in the liver, thus suggesting that organ heterogeneity is important in the pathogenesis of lung cancer metastasis. Organ heterogeneity in the therapeutic response is frequently observed in experimental xenograft models as well as in the clinical setting. Macrophage colony-stimulating factor gene transduction into human squamous cell lung carcinoma, RERF-LC-AI cells significantly suppresses experimental metastases in the liver but not the kidneys [13]. Treatment with, bevacizumab, an anti-human VEGF Ab, inhibits distant metastases of human ACC-LC-319/bone2 adenocarcinoma cells in the bone and the liver but not the lungs [14]. These observations imply that the heterogeneity of organ microenvironments affects the progression of lung cancer metastases.

The current experiments did not reveal why erlotinib failed to inhibit liver metastases, but one plausible explanation is that hepatocyte growth factor (HGF), which is produced by stromal cells in the liver as well as other organs, might be responsible for organ heterogeneity in the therapeutic response observed in this study. HGF acts as a potent mitogen for endothelial cells and binds to receptors expressed on endothelial cells, thus stimulating angiogenesis [39]. Yano et al. [40] demonstrated that HGF induces gefitinib resistance of lung adenocarcinoma cells with EGFR-activating mutations by restoring the phosphatidylinositol 3-kinase/Akt signaling pathway via phosphorylation of MET. These reports suggest that the microenvironment in the liver may not be favorable for EGFR–TKIs to exert antitumor activity. The current in vivo results also showed that erlotinib had therapeutic efficacy against lung metastases. Pulmonary vascular destabilization in the premetastatic phase promotes the extravasation of breast cancer cells and facilitates lung metastasis, indicating that vascular normalization might lead to the suppression of lung metastasis [41]. In addition, Cerniglia et al. [7] reported that erlotinib treatment with tumor-bearing mice alters vessel morphology and decreases vessel permeability in tumor xenografts, resulting in vascular normalization. Although erlotinib failed to show an inhibitory effect on tumor angiogenesis in this study, these findings indicate that EGFR–TKIs might prevent lung metastases by decreasing vessel permeability and preventing extravasation of tumor cells. Baker et al. [42] have previously reported that the EGFR expression of host cells such as endothelial cells is conditioned by tumor microenvironment. Thus, there is a possibility that EGFR expression status of SBC-5 cells might also be regulated by host organ microenvironment, although it is still unclear that EGFR expression of cancer cells is conditioned by

tumor microenvironment. Further studies are warranted to elucidate the mechanism of organ heterogeneity in the therapeutic response by erlotinib.

In summary, the current study demonstrated that erlotinib significantly suppressed bone and lung metastases by SBC-5 cells which did not express EGFR, while it had no inhibitory effect on the proliferation of SBC-5 cells in vitro. Even though the precise mechanisms remain uncertain, these results strongly suggested that erlotinib prevented distant metastasis formation by affecting host microenvironments irrespective of its direct effect on tumor cells. Erlotinib might therefore be a promising therapeutic candidate for the inhibition of distant metastases.

Acknowledgments This work was supported in part by a Grant-in-aid for Cancer Research from the Ministry of Education, Science, Sports and Culture of Japan, and Ministry of Health and Welfare of Japan.

References

1. Jemal A, Siegel R, Ward E, Hao Y, Xu J, Thun MJ (2009) Cancer statistics 2009. CA Cancer J Clin 59:225–249
2. Sone S, Yano S (2007) Molecular pathogenesis and its therapeutic modalities of lung cancer metastasis to bone. Cancer Metastasis Rev 26:685–689
3. Jackman DM, Yeap BY, Sequist LV, Lindeman N, Holmes AJ, Joshi VA, Bell DW, Huberman MS, Halmos B, Rabin MS, Haber DA, Lynch TJ et al (2006) Exon 19 deletion mutations of epidermal growth factor receptor are associated with prolonged survival in non-small cell lung cancer patients treated with gefitinib or erlotinib. Clin Cancer Res 12:3908–3914
4. Riely GJ, Pao W, Pham D, Li AR, Rizvi N, Venkatraman ES, Zakowski MF, Kris MG, Ladanyi M, Miller VA (2006) Clinical course of patients with non-small cell lung cancer and epidermal growth factor receptor exon 19 and exon 21 mutations treated with gefitinib or erlotinib. Clin Cancer Res 12:839–844
5. Mitsudomi T, Yatabe Y (2007) Mutations of the epidermal growth factor receptor gene and related genes as determinants of epidermal growth factor receptor tyrosine kinase inhibitors sensitivity in lung cancer. Cancer Sci 98:1817–1824
6. Normanno N, De Luca A, Aldinucci D, Maiello MR, Mancino M, D'Antonio A, De Filippi R, Pinto A (2005) Gefitinib inhibits the ability of human bone marrow stromal cells to induce osteoclast differentiation: implications for the pathogenesis and treatment of bone metastasis. Endocr Relat Cancer 12:471–482
7. Cerniglia GJ, Pore N, Tsai JH, Schultz S, Mick R, Choe R, Xing X, Durduran T, Yodh AG, Evans SM, Koch CJ, Hahn SM, Quon H, Sehgal CM, Lee WM, Maity A (2009) Epidermal growth factor receptor inhibition modulates the microenvironment by vascular normalization to improve chemotherapy and radiotherapy efficacy. PLoS ONE 4:6539–6549
8. Yano S, Nishioka Y, Izumi K, Tsuruo T, Tanaka T, Miyasaka M, Sone S (1996) Novel metastasis model of human lung cancer in SCID mice depleted of NK cells. Int J Cancer 67:211–217
9. Miki T, Yano S, Hanibuchi M, Sone S (2000) Bone metastasis model with multiorgan dissemination of human small-cell lung cancer (SBC-5) cells in natural killer cell-depleted SCID mice. Oncol Res 12:209–217
10. Miki T, Yano S, Hanibuchi M, Kanematsu T, Muguruma H, Sone S (2004) Parathyroid hormone-related protein (PTHrP) is responsible for production of bone metastasis, but not visceral metastasis, by human small cell lung cancer SBC-5 cells in natural killer cell-depleted SCID mice. Int J Cancer 108:511–515
11. Yano S, Zhang H, Hanibuchi M, Miki T, Goto H, Uehara H, Sone S (2003) Combined therapy with a new bisphosphonate, minodronate (YM529), and chemotherapy for multiple organ metastases of small cell lung cancer cells in severe combined immunodeficient mice. Clin Cancer Res 9:5380–5385
12. Yano S, Muguruma H, Matsumori Y, Goto H, Nakataki E, Edakuni N, Tomimoto H, Kakiuchi S, Yamamoto A, Uehara H, Ryan A, Sone S (2005) Antitumor vascular strategy for controlling experimental metastatic spread of human small cell lung cancer cells with ZD6474 in natural killer cell-depleted severe combined immunodeficiency mice. Clin Cancer Res 11:8789–8798
13. Yano S, Nishioka Y, Nokihara H, Sone S (1997) Macrophage colony-stimulating factor gene transduction into human lung cancer cells differentially regulates metastasis formations in various organ microenvironments of natural killer cell-depleted SCID mice. Cancer Res 57:784–790
14. Otsuka S, Hanibuchi M, Ikuta K, Yano S, Goto H, Ogino H, Yamada T, Kakiuchi S, Nishioka Y, Takahashi T, Sone S (2009) A bone metastasis model with osteolytic and osteoblastic properties of human lung cancer ACC-LC-319/bone2 in natural killer cell-depleted severe combined immunodeficient mice. Oncol Res 17:581–591
15. Kiura K, Watarai S, Shibayama T, Ohnoshi T, Kimura I, Yasuda T (1993) Inhibitory effects of cholera toxin on in vitro growth of human lung cancer cell lines. Anticancer Drug Des 8:417–428
16. Zhu J, Jia X, Xiao G, Kang Y, Partridge NC, Qin L (2007) EGF-like ligands stimulate osteoclastogenesis by regulating expression of osteoclast regulatory factors by osteoblasts: implications for osteolytic bone metastases. J Biol Chem 282:26656–26664
17. Tanaka T, Kitamura F, Nagasaka Y, Kuida K, Suwa H, Miyasaka M (1993) Selective long-term elimination of natural killer cells in vivo by an anti-interleukin 2 receptor β chain monoclonal antibody in mice. J Exp Med 178:1103–1107
18. Green LM, Reade JL, Ware CF (1984) Rapid colorimetric assay for cell viability: application to the quantitation of cytotoxic and growth inhibitory lymphokines. J Immunol Methods 70:257–268
19. van Erp NP, Gelderblom H, Guchelaar HJ (2009) Clinical pharmacokinetics of tyrosine kinase inhibitors. Cancer Treat Rev 35:692–706
20. Ogino A, Kitao H, Hirano S, Uchida A, Ishiai M, Kozuki T, Takigawa N, Takata M, Kiura K, Tanimoto M (2007) Emergence of epidermal growth factor receptor T790M mutation during chronic exposure to gefitinib in a non small cell lung cancer cell line. Cancer Res 67:7807–7814
21. Guillamo JS, Bouard SD, Valable S, Marteau L, Leuraud P, Marie Y, Poupon MF, Parienti JJ, Raymond E, Peschanski M (2009) Molecular mechanisms underlying effects of epidermal growth factor receptor inhibition of invasion, proliferation, and angiogenesis in experimental glioma. Clin Cancer Res 15:3697–3704
22. Riedel F, Götte K, Li M, Hörmann K, Grandis JR (2002) EGFR antisense treatment of human HNSCC cell lines down-regulates VEGF expression and endothelial cell migration. Int J Oncol 21: 11–16
23. Lipton A, Goessl C (2010) Clinical development of anti-RANKL therapies for treatment and prevention of bone metastasis. Bone 48:96–99
24. Fidler IJ, Kim SJ, Langley RR (2007) The role of the organ microenvironment in the biology and therapy of cancer metastasis. J Cell Biochem 101:927–936
25. Fidler IJ (2002) The organ microenvironment and cancer metastasis. Differentiation 70:498–505
26. Liotta LA, Kohn EC (2001) The microenvironment of the tumor-host interface. Nature 411:375–379

27. Langley RR, Fidler IJ (2007) Tumor cell-organ microenvironment interactions in the pathogenesis of cancer metastasis. Endocr Rev 28:297–321
28. Krampera M, Pasini A, Rigo A, Scupoli MT, Tecchio C, Malpeli G, Scarpa A, Dazzi F, Pizzolo G, Vinante F (2005) HB-EGF/HER-1 signaling in bone marrow mesenchymal stem cells: inducing cell expansion and reversibly preventing multilineage differentiation multilineage differentiation. Blood 106:59–66
29. Kim SM, Jung JU, Ryu JS, Jin JW, Yang HJ, Ko K, You HK, Jung KY, Choo YK (2008) Effects of gangliosides on the differentiation of human mesenchymal stem cells into osteoblasts by modulating epidermal growth factor receptors. Biochem Biophys Res Commun 371:866–871
30. Chien HH, Lin WL, Cho MI (2000) Down-regulation of osteoblastic cell differentiation by epidermal growth factor receptor. Calcif Tissue Int 67:141–150
31. Qin L, Tamasi J, Raggatt L, Li X, Feyen JH, Lee DC, Dicicco-Bloom E, Partridge NC (2005) Amphiregulin is a novel growth factor involved in normal bone development and in the cellular response to parathyroid hormone stimulation. J Biol Chem 280:3974–3981
32. Schneider MR, Sibilia M, Erben RG (2009) The EGFR network in bone biology and pathology. Trends Endocrinol Metab 20: 517–524
33. Furugaki K, Moriya Y, Iwai T, Yorozu K, Yanagisawa M, Kondoh K, Fujimoto-Ohuchi K, Mori K (2011) Erlotinib inhibits osteolytic bone invasion of human non-small-cell lung cancer cell line NCI-H292. Clin Exp Metastasis 28:649–659
34. Schwaninger R, Rentsch CA, Wetterwald A, van der Horst G, van Bezooijen RL, van der Pluijm G, Lowik CW, Ackermann K, Pyerin W, Hamdy FC, Thalmann GN, Cecchini MG (2007) Lack of noggin expression by cancer cells is a determinant of the osteoblast response in bone metastases. Am J Pathol 170:160–175
35. Wen YH, Koeppen H, Garcia R, Chiriboga L, Tarlow BD, Peters BA, Eigenbrot C, Yee H, Steiner G, Greco MA (2007) Epidermal growth factor receptor in osteosarcoma: expression and mutational analysis. Hum Pathol 38:1184–1191
36. Dobashi Y, Suzuki S, Sugawara H, Ooi A (2007) Involvement of epidermal growth factor receptor and downstream molecules in bone and soft tissue tumors. Hum Pathol 38:914–925
37. Di Lorenzo G, Tortora G, D'Armiento FP, De Rosa G, Staibano S, Autorino R, D'Armiento M, De Laurentiis M, De Placido S, Catalano G, Bianco AR, Ciardiello F (2002) Expression of epidermal growth factor receptor correlates with disease relapse and progression to androgen-independence in human prostate cancer. Clin Cancer Res 8:3438–3444
38. Kim SJ, Uehara H, Karashima T, Shepherd DL, Killion JJ, Fidler IJ (2003) Blockade of epidermal growth factor receptor signaling in tumor cells and tumor-associated endothelial cells for therapy of androgen-independent human prostate cancer growing in the bone of nude mice. Clin Cancer Res 9:1200–1210
39. Dunsmore SE, Rubin JS, Kovacs SO, Chedid M, Parks WC, Welgus HG (1996) Mechanisms of hepatocyte growth factor stimulation of keratinocyte metalloproteinase production. J Biol Chem 271:24576–24582
40. Yano S, Wang W, Li Q, Matsumoto K, Sakurama H, Nakamura T, Ogino H, Kakiuchi S, Hanibuchi M, Nishioka Y, Uehara H, Mitsudomi T et al (2008) Hepatocyte growth factor induces gefitinib resistance of lung adenocarcinoma with epidermal growth factor receptor-activating mutations. Cancer Res 68:9479–9487
41. Huang Y, Song N, Yanping Ding Y, Yuan S, Li X, Cai H, Shi H, Luo Y (2009) Pulmonary vascular destabilization in the premetastatic phase facilitates lung metastasis. Cancer Res 69:7529–7537
42. Baker CH, Keder D, McCarty MF, Tsan R, Weber KL, Bucana CD, Fidler IJ (2002) Blockade of epidermal growth factor receptor signaling on tumor cells and tumor-associated endothelial cells for therapy of human carcinomas. Am J Pathol 161:929–938

Axitinib plus gemcitabine versus placebo plus gemcitabine in patients with advanced pancreatic adenocarcinoma: a double-blind randomised phase 3 study

Hedy L Kindler, Tatsuya Ioka, Dirk J Richel, Jaafar Bennouna, Richard Létourneau, Takuji Okusaka, Akihiro Funakoshi, Junji Furuse, Young Suk Park, Shinichi Ohkawa, Gregory M Springett, Harpreet S Wasan, Peter C Trask, Paul Bycott, Alejandro D Ricart, Sinil Kim, Eric Van Cutsem

Lancet Oncol 2011; 12: 256–62
Published Online February 8, 2011
DOI:10.1016/S1470-2045(11)70004-3

See Comment page 206

University of Chicago Comprehensive Cancer Center, Chicago, IL, USA (H L Kindler MD); Osaka Medical Center for Cancer and Cardiovascular Diseases, Osaka, Japan (T Ioka MD); Academic Medical Centre, University of Amsterdam, Internal Medicine/Oncology, Amsterdam, Netherlands (D J Richel MD); Medical Oncology Services, Centre Rene Gauducheau, Nantes, France (J Bennouna MD); Centre Hospitalier, Universite de Montreal, Montreal, QC, Canada (R Létourneau MD); National Cancer Center Hospital, Tokyo, Japan (T Okusaka MD); National Kyushu Cancer Center, Department of Gastroenterology, Fukuoka, Japan (A Funakoshi MD); National Cancer Center Hospital East, Chiba, Japan (J Furuse MD); Divisions of Hematology-Oncology, Department of Medicine, Samsung Medical Center, Sungkyunkwan University School of Medicine, Seoul, South Korea (Y S Park MD); Kanagawa Cancer Center Hospital, Hepatobiliary and Pancreatic Oncology, Yokohama, Japan (S Ohkawa MD); H Lee Moffitt Cancer Center and Research Institute, Department of Gastrointestinal Oncology, WCB-GI Program, Tampa, FL, USA (G M Springett MD); Hammersmith Hospital, Department of Cancer Medicine, London, UK (H S Wasan MB); Pfizer Oncology, New London, CT, USA (P C Trask PhD); Pfizer Oncology, Pfizer Global Research and Development,

Summary

Background **Axitinib is a potent, selective inhibitor of vascular endothelial growth factor (VEGF) receptors 1, 2, and 3. A randomised phase 2 trial of gemcitabine with or without axitinib in advanced pancreatic cancer suggested increased overall survival in axitinib-treated patients. On the basis of these results, we aimed to assess the effect of treatment with gemcitabine plus axitinib on overall survival in a phase 3 trial.**

Methods **In this double-blind, placebo-controlled, phase 3 study, eligible patients had metastatic or locally advanced pancreatic adenocarcinoma, no uncontrolled hypertension or venous thrombosis, and Eastern Cooperative Oncology Group performance status 0 or 1. Patients, stratified by disease extent (metastatic *vs* locally advanced), were randomly assigned (1:1) to receive gemcitabine 1000 mg/m² intravenously on days 1, 8, and 15 every 28 days plus either axitinib or placebo. Axitinib or placebo were administered orally with food at a starting dose of 5 mg twice a day, which could be dose-titrated up to 10 mg twice daily if well tolerated. A centralised randomisation procedure was used to assign patients to each treatment group, with randomised permuted blocks within strata. Patients, investigators, and the trial sponsor were masked to treatment assignments. The primary endpoint was overall survival. All efficacy analyses were done in all patients assigned to treatment groups for whom data were available; safety and treatment administration and compliance assessments were based on treatment received. This study is registered at ClinicalTrials.gov, number NCT00471146.**

Findings **Between July 27, 2007, and Oct 31, 2008, 632 patients were enrolled and assigned to treatment groups (316 axitinib, 316 placebo). At an interim analysis in January, 2009, the independent data monitoring committee concluded that the futility boundary had been crossed. Median overall survival was 8·5 months (95% CI 6·9–9·5) for gemcitabine plus axitinib (n=314, data missing for two patients) and 8·3 months (6·9–10·3) for gemcitabine plus placebo (n=316; hazard ratio 1·014, 95% CI 0·786–1·309; one-sided p=0·5436). The most common grade 3 or higher adverse events for gemcitabine plus axitinib and gemcitabine plus placebo were hypertension (20 [7%] and 5 [2%] events, respectively), abdominal pain (20 [7%] and 17 [6%]), fatigue (27 [9%] and 21 [7%]), and anorexia (19 [6%] and 11 [4%]).**

Interpretation **The addition of axitinib to gemcitabine does not improve overall survival in advanced pancreatic cancer. These results add to increasing evidence that targeting of VEGF signalling is an ineffective strategy in this disease.**

Funding **Pfizer.**

Introduction

The prognosis for patients with advanced pancreatic adenocarcinoma is poor, and gemcitabine, the standard of care, offers only slight benefit.[1,2] Despite extensive research, combination regimens with gemcitabine and cytotoxic or molecularly targeted agents have not significantly improved outcomes compared with gemcitabine monotherapy.[3] The addition of erlotinib to gemcitabine resulted in a significant but very small improvement in overall survival.[3,4] There is a pressing need for new treatment options for this disease.

Axitinib is an oral, potent, and selective inhibitor of vascular endothelial growth factor (VEGF) receptors 1, 2, and 3.[5] A randomised phase 2 study[6] of 103 patients with locally advanced and metastatic pancreatic adenocarcinoma showed an improvement in median overall survival (6·9 *vs* 5·6 months; hazard ratio [HR] 0·71, 95% CI 0·44–1·13) and a greater 1-year survival (37% *vs* 24%) for axitinib plus gemcitabine versus gemcitabine alone. Although not significant, the apparent increase in survival in the combination group provided the rationale for a larger phase 3 study of this regimen. We aimed to assess overall survival in patients with advanced pancreatic cancer treated with gemcitabine plus axitinib versus gemcitabine plus placebo.

Methods

Study design and patients

We undertook a phase 3, randomised, double-blind, global, multicentre, two-group study. Eligible patients were at least 18 years old with histologically or cytologically confirmed metastatic or locally advanced pancreatic adenocarcinoma not amenable to curative resection. Patients were required to have adequate bone marrow, hepatic, and renal function (including urine protein <2 g/24 h); an Eastern Cooperative Oncology Group (ECOG) performance status of 0 or 1; and no uncontrolled hypertension (two baseline blood pressure readings ≤140/90 mm Hg). Patients with documented

invasion of adjacent hollow organs were excluded. Adjuvant therapy that did not contain gemcitabine was allowed if 4 weeks or longer had passed since the last dose; previous radiation was allowed if there was disease outside the radiation port. Additional exclusion factors included: previous treatment with VEGF or VEGF receptor inhibitors; previous systemic chemotherapy for locally advanced or metastatic disease; use of a thrombolytic agent within 1 month of treatment; central lung lesions involving major blood vessels; recent haemoptysis, myocardial infarction, symptomatic congestive heart failure, cerebrovascular accident, transient ischaemic attack, deep-vein thrombosis, or pulmonary embolism in the past 12 months; peptic ulcer disease needing treatment in the past 6 months; active seizures or gastrointestinal bleeding; malabsorption syndromes; present use of potent cytochrome P450 (CYP) 3A4 inhibitors or CYP3A4 or CYP1A2 inducers; or major surgery within 4 weeks.

The study was undertaken with institutional review board approval and in accordance with the International Conference on Harmonisation Good Clinical Practice guidelines, as well as applicable local laws and regulatory requirements. All patients provided written informed consent.

Randomisation and masking

Patients were stratified by disease extent (metastatic *vs* locally advanced) and randomly allocated in a 1:1 ratio to receive gemcitabine plus either axitinib or placebo. A centralised randomisation procedure (interactive voice randomisation system accessible via telephone or internet) was used to assign patients to each treatment group, with randomised permuted blocks within strata. Randomisation was not done by centre, but by stratification category, and use of blocked randomisation made guessing of the next treatment assignment within a block almost impossible. Patients, investigators, and the trial sponsor were masked to treatment assignments.

Procedures

All patients received gemcitabine 1000 mg/m^2 intravenously during 30 min on days 1, 8, and 15 of each 4-week treatment cycle until disease progression, unacceptable toxic effects, or withdrawal of consent. Dose reductions to 750 mg/m^2, 550 mg/m^2, and 425 mg/m^2 were allowed for management of adverse events. Gemcitabine was discontinued in patients needing a dose interruption longer than 4 weeks or a dose reduction to less than 425 mg/m^2.

All patients also received either axitinib or placebo, administered orally with food at a starting dose of 5 mg twice a day, which was continued until disease progression, unacceptable toxic effects, or withdrawal of consent. Stepwise dose increases to 7 mg and then 10 mg twice a day were allowed in the absence of axitinib-related or placebo-related grade 3 or higher adverse events for consecutive 2-week periods in patients with blood pressure 150/90 mm Hg or lower who were not receiving antihypertensive drugs. Dose reductions to 3 mg or 2 mg twice daily were allowed for management of adverse events. In patients with systolic blood pressure higher than 150 mm Hg or diastolic blood pressure higher than 100 mm Hg, new or additional antihypertensive treatment was initiated and axitinib or placebo was continued. For patients on maximum antihypertensive treatment, the axitinib or placebo dose was reduced one level. For systolic blood pressure higher than 160 mm Hg or diastolic blood pressure higher than 105 mm Hg, antihypertensive treatment was adjusted, and axitinib or placebo dosing was interrupted and resumed at one lower dose level once blood pressure was lower than 150/100 mm Hg. If proteinuria of 2 g per day or higher occurred, axitinib or placebo dosing was interrupted and resumed at one lower dose level once proteinuria less than 2 g per day was recorded. For all other grade 3 axitinib-related or placebo-related non-haematological adverse events, the axitinib or placebo dose was decreased by one level. For grade 4 axitinib-related or placebo-related non-haematological adverse events or grade 4 haematological adverse events (except lymphopenia), dosing was interrupted and resumed at one lower dose level when the adverse event improved to grade 2 or lower. Treatment was discontinued if a dose interruption for longer than 4 weeks or a dose reduction to less than 2 mg twice a day was needed. If either gemcitabine or axitinib/placebo was interrupted or withdrawn, the remaining therapy was continued.

CT scans were obtained at screening, every 8 weeks during the study, and at follow-up 28 days after the last dose in patients who discontinued without progressive disease. Tumour response was assessed using the Response Evaluation Criteria in Solid Tumours (RECIST).[7] Safety was monitored by physical examination, urinalysis, haematology, and clinical chemistry tests; assessment of ECOG performance status; and adverse event reporting, based on the National Cancer Institute Common Terminology Criteria for Adverse Events (CTCAE), version 3.0. An independent data monitoring committee reviewed accumulating unmasked safety and survival data during the study. Blood pressure was monitored in the clinic at baseline, on days 1, 8, and 15 of each 4-week treatment cycle, and at follow-up. Blood pressure was also measured and recorded in diaries by patients before each dose of axitinib or placebo. Thyroid-stimulating hormone (TSH) concentrations were evaluated at baseline, every 2 weeks for the first 6 weeks, and every 8 weeks thereafter.

The primary endpoint was overall survival; secondary endpoints included progression-free survival, objective response rate, duration of response, safety, and health-related quality of life. Health-related quality of life, pancreatic cancer-specific symptoms, pain, and health status were measured with the European Organisation for the Research and Treatment of Cancer quality of life questionnaire–core 30 (QLQ-C30) and pancreatic cancer module (QLQ-PAN26) at baseline, on day 1 of each treatment cycle, and 28 days after the last dose.[8,9]

La Jolla Laboratories, San Diego, CA, USA (P Bycott PhD, A D Ricart MD, S Kim MD); **and University Hospital Gasthuisberg/Leuven, Department of Digestive Oncology, Leuven, Belgium** (E Van Cutsem MD)

Correspondence to:
Dr Hedy L Kindler, Section of Hematology/Oncology, University of Chicago, Chicago, IL 60637, USA
hkindler@medicine.bsd.uchicago.edu

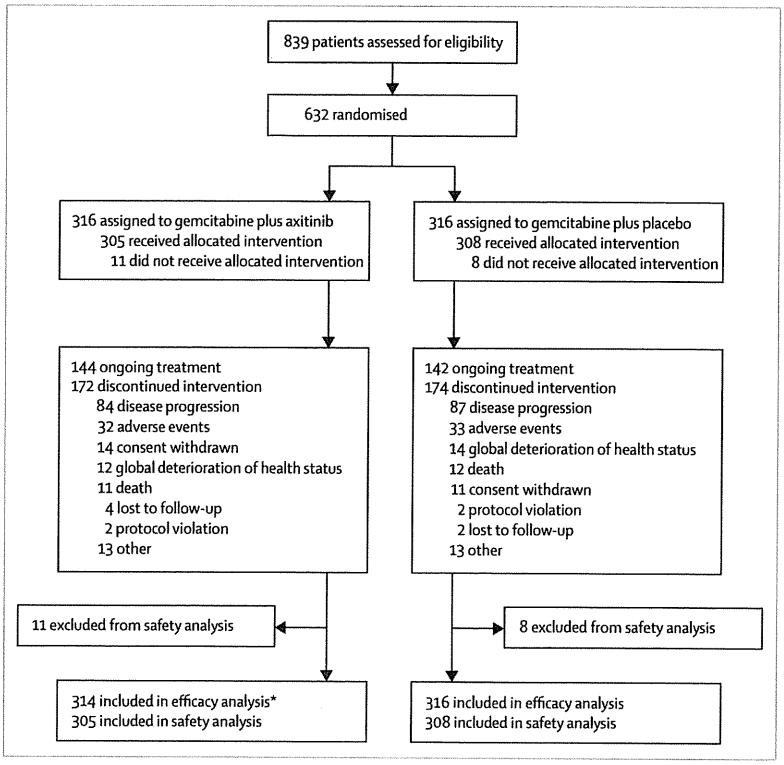

Figure 1: **Trial profile**
*Data missing from database at time of analysis for two patients.

	Axitinib plus gemcitabine (n=314)*	Placebo plus gemcitabine (n=316)
Median age (years)	61 (34–84)	62 (35–89)
Sex		
Male	191 (61%)	188 (59%)
Female	123 (39%)	128 (41%)
ECOG performance status		
0	147 (47%)	158 (50%)
1	162 (52%)	154 (49%)
Missing	5 (2%)	4 (1%)
Disease extent		
Locally advanced	77 (25%)	73 (23%)
Metastatic	226 (72%)	227 (72%)
Missing	11 (4%)	16 (5%)
Metastatic sites		
Liver	146/264 (55%)	135/263 (51%)
Lung	63/264 (24%)	57/263 (22%)
Peritoneum	16/264 (6%)	20/263 (8%)
Previous adjuvant chemotherapy†	12 (4%)	12 (4%)
Mean QLQ-30 global health status/QoL score	54·2 (22·3)‡	57·1 (23·1)§

Data are median (range), n/N (%), or mean (SD). Some data are missing from this table because they were derived from case report forms. ECOG=Eastern Cooperative Oncology Group. QLQ-C30=European Organisation for the Research and Treatment of Cancer quality of life questionnaire, core 30. QoL=quality of life. *Data missing from database at time of analysis for two patients. †Includes neoadjuvant therapy. ‡Data missing from database at time of analysis for 22 patients. §Data missing from database at time of analysis for 28 patients.

Table 1: **Baseline characteristics**

Questionnaires were completed in the clinic before interaction with health-care personnel.

Statistical analysis

On the assumption of a 36·7% improvement in median overall survival from 6 months to 8·2 months in patients allocated axitinib plus gemcitabine and non-uniform accrual (roughly 40% of patients enrolled at 7 months), 460 deaths were needed for a log-rank test with an overall one-sided significance level of 0·025 to have a power of 0·90. The assumed improvement in median overall survival was based on results available from the randomised phase 2 trial[6] at the time that this phase 3 study was designed. Applying a 1:1 randomisation, a planned accrual period of 14 months, and a follow-up of roughly 9 months, we estimated that 596 patients would need to enrol to provide 460 deaths. The nominal significance level for the interim futility and efficacy analysis was established with the Pampallona-Tsiatis power boundary and the Lan-DeMets procedure with an O'Brien-Fleming stopping boundary, respectively.[10,11] SAS (version 9.1.3) was used for all analyses.

The primary endpoint of overall survival and other secondary efficacy endpoints were analysed in all patients randomly assigned to treatment groups for whom data were available. Safety and treatment administration and compliance assessments were based on the treatment received. Overall survival was a time-to-event outcome, defined as the time from date of randomisation to date of death from any cause. Objective response rate was defined as the percentage of patients with a confirmed complete or partial response (RECIST). Duration of response was a time-to-event outcome, defined as the time from first documentation of objective tumour response that was subsequently confirmed to first documentation of disease progression or to death from any cause. Time-to-event analyses were done with the Kaplan-Meier method[12] and compared with a one-sided stratified log-rank test at the α=0·025 significance level (the log-rank test was stratified by disease extent [metastatic *vs* locally advanced]); Cox proportional-hazards models were used to explore the effect of baseline characteristics on survival. We compared the proportion of patients with an objective response in each treatment group with a significance level of 0·025 using a one-sided Pearson χ^2 test for unstratified analyses and Cochran-Mantel-Haenszel test for stratified analyses. One-sided significance tests were used because interest centred on whether axitinib plus gemcitabine improved clinical outcomes compared with placebo plus gemcitabine. An interim analysis was planned after roughly half (230) of the deaths had taken place and occurred on Jan 23, 2009.

This study is registered with ClinicalTrials.gov, number NCT00471146.

Role of the funding source

The study was designed by the corresponding author in consultation with the study sponsor. The study sponsor

managed all logistical aspects of the study and collected data. Data analysis was done by the sponsor in collaboration with the global team of academic investigators. All authors had full access to the data, and the corresponding author had final responsibility to submit for publication.

Results

Between July 27, 2007, and Oct 31, 2008, 632 patients were randomly assigned to treatment groups (316 to each group). 305 patients in the gemcitabine plus axitinib group and 308 in the gemcitabine plus placebo group received study treatment (figure 1). The baseline characteristics of the treatment groups seemed well balanced (table 1). Most patients (226 [72%] in the gemcitabine plus axitinib and 227 [72%] in the gemcitabine plus placebo group) had metastatic disease and about half had an ECOG performance status of 1.

The median duration of axitinib treatment was 2·8 months (range 0·03–11·0); the median relative dose intensity (actual total dose/intended total dose) was 100%, with the intended total axitinib dose based on 5 mg twice a day. The median duration of gemcitabine exposure was 2·3 months (range 0·03–11·1) with a median relative dose intensity of 77% in combination with axitinib, versus 2·4 months (0·03–11·8) and 79%, respectively, with placebo. The median number of gemcitabine treatment cycles was three in both groups (range 1–13 for gemcitabine plus axitinib, 1–12 for gemcitabine plus placebo). Dose reductions of axitinib or placebo occurred in 74 (25%) of 298 patients in the axitinib group versus 30 (10%) of 301 patients on the placebo group. Axitinib dose titration to more than 5 mg twice daily occurred in 95 (32%) of 298 patients (range 12–20 mg total daily dose), and 36 (12%) of 298 subsequently needed dose reductions. The dose titrations of axitinib to more than 5 mg twice a day led to a median relative dose intensity of 100%, despite dose reductions occurring in 25% of patients.

At a planned interim analysis in January, 2009, the independent data monitoring committee concluded that the futility boundary had been crossed. Patients on treatment were notified, treatment assignments were unmasked, and discontinuation of axitinib was recommended.

Median follow-up for the gemcitabine plus placebo group was 27 weeks (range 0·1–51·7) and for gemcitabine plus axitinib was 27·4 weeks (0·1–55·5). Median overall survival in the efficacy population was similar in both treatment groups: 8·5 months (95% CI 6·9–9·5) for patients allocated axitinib plus gemcitabine and 8·3 months (6·9–10·3) for those allocated placebo plus gemcitabine (HR 1·014, 95% CI 0·786–1·309; Cox model, one-sided p=0·5436, stratified log-rank test; table 2, figure 2). Median progression-free survival, at 4·4 months, was the same for both treatment groups (HR 1·006, 95% CI 0·779–1·298; one-sided p=0·5203; table 2, figure 2).

Disease stage and ECOG performance status, but not treatment, were strong independent predictors of overall survival (Cox proportional-hazards model; table 3). As expected, patients with locally advanced disease lived longer than did those with metastatic disease, and

	Axitinib plus gemcitabine	Placebo plus gemcitabine	Hazard ratio (95% CI)	One-sided p value
Best response*				
Overall objective response rate	12 (5%, 2·5–8·3)	4 (2%, 0·4–4·0)	..	0·0180
Complete response	1 (<1%)	0	..	..
Partial response	11 (4%)	4 (2%)	..	..
Stable disease	74 (30%)	83 (33%)	..	..
Median survival (months)†				
Overall survival	8·5 (6·9–9·5)	8·3 (6·9–10·3)	1·014 (0·786–1·309)	0·5436
Locally advanced	9·5 (7·4–NR)	10·6 (9·9–NR)	..	..
Metastatic	7·0 (5·8–9·3)	6·9 (6·2–8·0)	..	..
Progression-free survival	4·4 (4·0–5·6)	4·4 (3·7–5·2)	1·006 (0·779–1·298)	0·5203
Locally advanced	5·9 (4·2–7·3)	9·1 (5·8–10·6)	..	..
Metastatic	4·2 (3·7–5·4)	3·8 (3·6–4·5)	..	..

Data for best response are n (%, 95% CI); data for survival are median (95% CI). NR=not reached. *Only patients with measurable disease at baseline were included in the analysis; n=247 for axitinib plus gemcitabine, n=255 for placebo plus gemcitabine. †Analysis included all patients randomly assigned to treatment groups; n=314 for axitinib plus gemcitabine (data missing from database at time of analysis for two patients), n=316 for placebo plus gemcitabine.

Table 2: **Efficacy results**

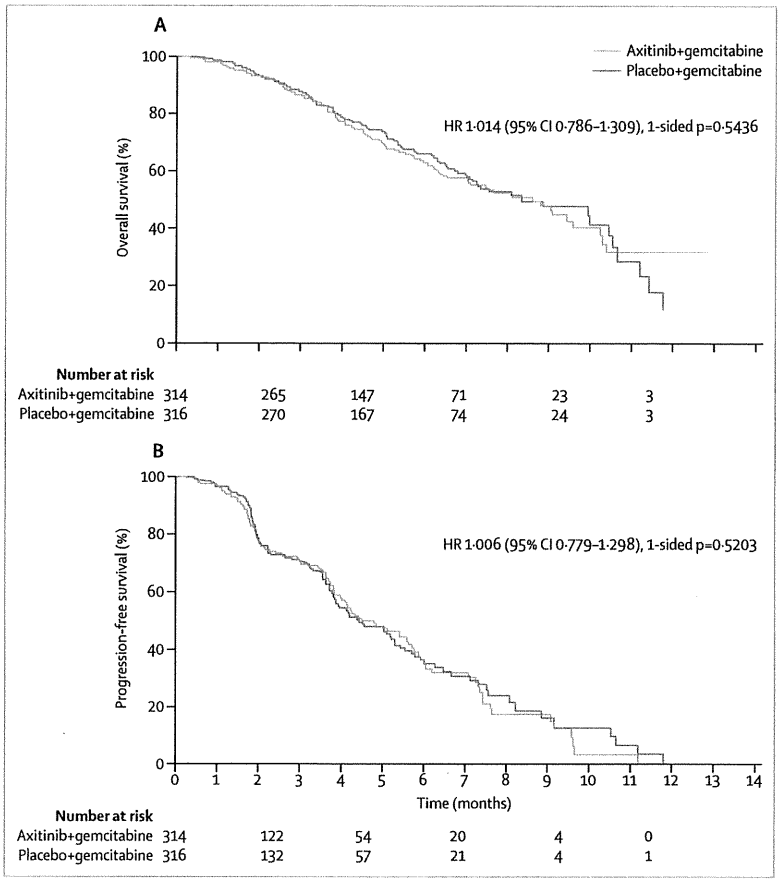

Figure 2: **Kaplan-Meier estimates of (A) overall survival and (B) progression-free survival**

patients with a performance status of 0 lived longer than did those with a status of 1.

502 patients (247 and 255 in the axitinib and placebo groups, respectively) had measurable disease at baseline and could be evaluated for response. The overall objective response rate was 12 (5%) of 247 patients receiving axitinib plus gemcitabine and four (2%) of 255 patients receiving placebo plus gemcitabine (one-sided p=0·0180; table 2). Stable disease was achieved in 74 (30%) of 247 and 83 (33%) of 255 patients in the axitinib and placebo groups, respectively.

	Hazard ratio (95% CI)	p value*
Treatment (axitinib plus gemcitabine *vs* placebo plus gemcitabine)	0·994 (0·770–1·284)	0·9657
Disease stage (locally advanced *vs* metastatic)	0·433 (0·301–0·623)	<0·0001
ECOG performance status (0 *vs* 1)	0·497 (0·380–0·650)	<0·0001

The initial Cox model included baseline factors significant at the 0·10 level in the individual analyses. Backward stepwise selection using an α level of 0·05 was then used to create the final model while forcing treatment to stay in the model/results. ECOG=Eastern Cooperative Oncology Group. *p values are two-sided (Wald χ^2 test).

Table 3: **Multivariate Cox model analysis of overall survival**

	Axitinib plus gemcitabine (n=305)		Placebo plus gemcitabine (n=308)	
	Grade 1 or 2	Grade ≥3	Grade 1 or 2	Grade ≥3
Non-haematological events				
Nausea	129 (42%)*	13 (4%)	106 (34%)	8 (3%)
Fatigue	100 (33%)	27 (9%)	94 (31%)	21 (7%)
Diarrhoea	97 (32%)*	4 (1%)	63 (20%)	5 (2%)
Anorexia	95 (31%)*	19 (6%)	73 (24%)	11 (4%)
Vomiting	86 (28%)	12 (4%)	92 (30%)	10 (3%)
Constipation	85 (28%)	3 (1%)	89 (29%)	7 (2%)
Dysphonia	67 (22%)*	1 (<1%)	13 (4%)	0
Hypertension	65 (21%)*	20 (7%)*	22 (7%)	5 (2%)
Stomatitis	52 (17%)*	0	11 (4%)	1 (<1%)
Pyrexia	47 (15%)	3 (1%)	47 (15%)	1 (<1%)
Abdominal pain	43 (14%)	20 (7%)	41 (13%)	17 (6%)
Peripheral oedema	23 (8%)	0	48 (16%)*	2 (1%)
Haematological abnormalities				
Neutropenia	0	0	3 (1%)	1 (<1%)
Thrombocytopenia	16 (5%)	0	16 (5%)	1 (<1%)
Anaemia	131 (43%)	0	151 (49%)	2 (1%)
Leucopenia	8 (3%)*	0	18 (6%)	0
Lymphopenia	28 (9%)	3 (1%)	42 (14%)	2 (1%)

Data are n (%). *Significant difference in frequency between treatment groups (two-sided 95% CIs exclude 0 for risk differences and 1 for risk ratios).

Table 4: **Adverse events (all causes) reported in 15% or more of patients, and haematological laboratory abnormalities**

	Axitinib plus gemcitabine (n=305)	Placebo plus gemcitabine (n=308)
Asthenia	16 (5%)*†	6 (2%)
Gastrointestinal perforation	4 (1%)	2 (1%)*
Pulmonary embolism	4 (1%)	7 (2%)
Deep-vein thrombosis	4 (1%)	8 (3%)
Gastrointestinal bleeding	2 (1%)	5 (2%)
Cerebrovascular accident	1 (<1%)	1 (<1%)
Proteinuria	1 (<1%)	0

Data are n (%). VEGF=vascular endothelial growth factor. *Includes one grade 5 event. †Significant difference in frequency between treatment groups (two-sided 95% CIs exclude 0 for risk differences and 1 for risk ratios).

Table 5: **Non-haematological grade 3 or 4 adverse events (all causes) attributable to VEGF inhibition or of clinical interest**

Table 4 shows the most common adverse events of any cause, by maximum CTCAE grade. Non-haematological adverse events attributable to VEGF inhibition are presented in table 5. Nausea, diarrhoea, anorexia, dysphonia, hypertension, and stomatitis occurred more frequently in patients receiving axitinib and gemcitabine; peripheral oedema occurred more frequently in patients receiving placebo. Grade 3 or 4 asthenia and hypertension occurred more often in patients on axitinib. Overall, there were two grade 5 events in the placebo group (one cardiac arrest and one cardiac failure) and five in the axitinib group (one each of interstitial lung disease, gastrointestinal haemorrhage, asthenia, acute renal failure, and death).

Grade 3 or 4 deep-vein thrombosis or pulmonary embolism developed in eight (3%) of 305 patients who received axitinib and gemcitabine and 15 (5%) of 308 patients receiving placebo and gemcitabine. Grade 3 or 4 gastrointestinal perforation occurred in four (1%) patients receiving axitinib plus gemcitabine and in two (1%) receiving placebo plus gemcitabine (table 5), mostly associated with tumour involving the bowel wall. Grade 3 or 4 gastrointestinal haemorrhage, probably related to underlying disease, developed in two (1%) patients who received axitinib plus gemcitabine and five (3%) who received placebo plus gemcitabine (table 5).

At study entry, normal concentrations of TSH (<5 μU/mL) were noted in 104 (91%) of 114 patients in the axitinib group and 123 (93%) of 132 patients in the placebo group. Post-treatment increases of TSH (≥5 μU/mL) occurred in 48 (42%) of 114 patients receiving axitinib and gemcitabine and 15 (11%) of 132 patients receiving placebo and gemcitabine, and hypothyroidism as an adverse event was reported in 18 (6%) of 305 patients in the axitinib group and four (1%) of 308 patients taking placebo. 13 of 18 patients who developed hypothyroidism on axitinib plus gemcitabine had asthenia or fatigue, or both, including four grade 3 or 4 cases.

At baseline, the mean scores on the global health status/quality of life scale of the QLQ-C30 did not differ significantly between the two groups (table 1). For patients with a baseline and cycle 4, day 1, value for the global health status scale, after three cycles the mean difference from baseline was 0·1 (n=132) for axitinib plus gemcitabine and 2·8 (n=132) for the placebo group. Patients in the axitinib and gemcitabine group reported a 5-point or more mean change from baseline in pain, constipation, insomnia, and financial difficulties (all improved), and physical functioning, dyspnoea, diarrhoea, and fatigue (all worsened) on the QLQ-C30; on the QLQ-PAN26, patients who received axitinib and gemcitabine reported